The Gödel universe: Exact geometrical optics and analytical investigations on motion

Frank Grave,[1, 2, *] Michael Buser,[3] Thomas Müller,[2] Günter Wunner,[1] and Wolfgang P. Schleich[3]

[1] *1. Institut für Theoretische Physik, Universität Stuttgart, Pfaffenwaldring 57 // IV, 70550 Stuttgart, Germany*
[2] *Visualisierungsinstitut der Universität Stuttgart, Universität Stuttgart, Nobelstraße 15, D-70569 Stuttgart, Germany*
[3] *Institut für Quantenphysik, Universität Ulm, D-89069 Ulm, Germany*

(Dated: October 16, 2009)

In this work we derive the analytical solution of the geodesic equations of Gödel's universe for both particles and light in a special set of coordinates which reveals the physical properties of this spacetime in a very transparent way. We also recapitulate the equations of isometric transport for points and derive the solution for Gödel's universe. The equations of isometric transport for vectors are introduced and solved. We utilize these results to transform different classes of curves along Killing vector fields. In particular, we generate non-trivial closed timelike curves (CTCs) from circular CTCs. The results can serve as a starting point for egocentric visualizations in the Gödel universe.

PACS numbers: 95.30.Sf, 04.20.-q, 04.20.Ex, 04.20.Fy, 04.20.Gz, 04.20.Jb

I. INTRODUCTION

Gödel's cosmological solution of Einstein's field equations, published in 1949 [1], represents a basic model of a "rotating universe" with negative cosmological constant Λ. Its spacetime curvature originates from a homogeneous matter distribution which rotates around every point with a constant rotation rate. The energy momentum tensor consists of an ideal fluid whose pressure and mass density are connected to the cosmological constant and the rotation scalar of Gödel's universe [2].

A particularly puzzling feature of Gödel's universe is the existence of closed timelike curves (CTCs). Gödel himself was the first who pointed out their existence within the framework of general relativity, although the van Stockum dust cylinder model of 1937 already possesses CTCs [3]. Besides Gödel's universe and the van Stockum dust cylinder, numerous other spacetimes have been found, which allow for time travel, such as the Kerr metric [4], the Gott universe of two cosmic strings [4, 5], various wormhole spacetimes [6], or two massive particles in a $(2+1)$-dimensional anti-de-Sitter spacetime [7]. Over the last decades, these metrics stimulated many discussions on the philosophical consequences of time travel and causality violations within the theory of relativity. In particular, Hawking established the so-called chronology protection conjecture which states that the laws of nature prevent time travel on all but sub-microscopic scales [8].

Gödel's metric facilitates analytical investigations, because it is highly symmetric and possesses five independent Killing vector fields. Already Gödel himself took advantage of four isometry groups to show that his cosmological solution is spacetime homogeneous [1]. A more detailed examination of the Killing fields was later performed by Navez [9]. He showed that Gödel's universe is endowed with five independent Killing vector fields and he examined the structure of the corresponding Lie algebra. The Killing equations for Gödel-type spacetimes were also discussed by Raychaudhuri et. al. [10]. They derived the necessary conditions for Gödel-type metrics to inherit at least four independent Killing vector fields – constituting the minimum requirement to satisfy the homogeneity of the spacetime. Based upon this work, and independent of Naves' work [9], Rebouças et. al. [11] showed that these conditions lead to five independent Killing vector fields. We note that Barrow and Tsagas [12] investigated the stability of Gödel's solution with respect to scalar, vector, and tensor perturbation modes using a gauge covariant formalism.

Gödel's universe is one of the simplest solutions of Einstein's field equations which allows for CTCs. As pointed out by Gödel [1] there exist geometrically very simple CTCs corresponding to "circular orbits" in specific coordinates which display the rotational symmetry of the metric most clearly. These circular orbits were also discussed by Raychaudhuri et. al. [10] and Pfarr [13], who categorized them into CTCs, coordinate dependent past-traveling curves (PTCs) and closed null curves (CNCs). Rosa and Letelier [14] analyzed the stability of CTCs under tiny changes of the energy momentum tensor. However, these circular orbits are not the only possible CTCs in Gödel's universe, see e. g. Sahdev et. al. [15].

The geodesic equations for Gödel's metric have been examined in several works so far. They were first solved in 1956 by Kundt [16], who took advantage of the Killing vectors and the corresponding constants of motion. In 1961, Chandrasekhar and Wright [17] presented an independent derivation of the solution. They concluded that there are no closed timelike geodesics and noted that this

*Electronic address: frank.grave@vis.uni-stuttgart.de; URL: http://www.vis.uni-stuttgart.de/~grave

fact seems to be contrary to Gödel's statement that the "circular orbits" allow one "to travel into the past, or otherwise influence the past". Nine years later, Stein [18] pointed out that the "circular orbits" of Gödel are by no means geodesics and that Chandrasekhar's and Wright's conclusion was incorrect, see also [19]. Other detailed studies of the geodesics in Gödel's universe followed by Pfarr [13] and Novello et. al. [20]. The latter provided a detailed discussion on geodesical motion using the effective potential as well as the analytical solution. They already assumed that any geodesic can be generated from geodesics starting at the origin by a suitable isometric transformation.

The understanding of null geodesics provides the bedrock for ray tracing in Gödel's spacetime. Egocentric visualizations of certain scenarios in Gödel's universe can be found in our previous work [21]. There, we presented improvements for visualization techniques regarding general relativity. Furthermore, finite isometric transformations were used to visualize illuminated objects. This method was technically reworked and improved in [22] and resulted in an interactive method for visualizing various aspects of Gödel's universe from an egocentric perspective. In that work, we used the analytical solution to the geodesic equations and a numerical integration of the equations of isometric transport.

This paper is organized as follows. In Sec. II A, we review several basic characteristics of Gödel's universe to make this work self-contained. The equations of motion are summarized and the constants of motion are expressed with respect to a local frame of reference. All Killing vector fields are specified as well. We follow the notation of Kajari et. al. [2] because we regard their choice of a set of coordinates as highly suitable and easily interpretable. Sec. III details the solution to the geodesic equations for timelike and lightlike motion. After discussing the special case of geodesics starting at the origin, we introduce the general solution and explain under which circumstances time travel on geodesics is possible. In Sec. IV, we derive analytical expressions on finite isometric transformations along Killing vector fields for points as well as directions. All results are then used in Sec. V to isometrically transform initial conditions for geodesics to map the special solution of the geodesic equations onto the general solution. Also, the Gödel horizon is calculated for different observers at rest with respect to the rotating matter and depicted for our choice of coordinates. Finally, we carry out a detailed analysis of circular CTCs and use finite isometric transformations to generate a class of non-circular CTCs. In the appendix, we describe several details on the solution to the geodesic equations and equations of isometric transport for easier reproduction of our results by the reader. The last section in the appendix provides interesting estimates of our results using astronomical data.

II. GÖDEL'S UNIVERSE

A. Basic properties

For the reader's convenience we recapitulate a few basic features of Gödel's universe. For details we refer, e. g., to the work of Kajari et. al. [2] or Feferman [23]. The line element of Gödel's universe in cylindrical coordinates [2], with the velocity of light c and the Gödel radius r_G, reads

$$\begin{aligned} ds^2 &= -c^2dt^2 + \frac{dr^2}{1+(r/r_G)^2} + r^2\left[1-(r/r_G)^2\right]d\varphi^2 \\ &\quad + dz^2 - \frac{2\sqrt{2}r^2c}{r_G}dtd\varphi, \end{aligned} \tag{1}$$

when using a positive signature of the metric tensor, i. e. $\mathrm{sign}(g_{\mu\nu})=+2$. This convention will be used throughout the paper. Furthermore, initial conditions for positions and directions are always denoted by a lower index of zero, i. e. $x^\mu(0) = x_0^\mu$ and $u^\mu(0) = u_0^\mu$.

Gödel's universe describes [1] a homogeneous universe, in which matter rotates everywhere clockwise with a constant angular velocity relative to the compass of inertia. It can easily be shown that, in this reference frame, massive particles with zero initial velocity propagate only in time. Hence, these cylindrical coordinates are corotating with the matter.

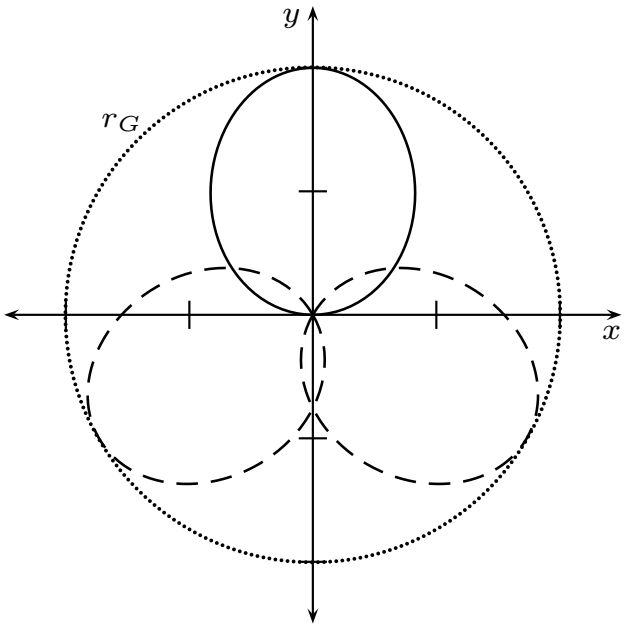

FIG. 1: Lightlike geodesics in the (xy)-subspace depicted in pseudo-Cartesian coordinates (cf. Fig. 2 in [2]). Photons emitted at the origin propagate counterclockwise into the future, reach a maximum radial distance of r_G, and then return to the origin. It can be shown that there exists no causality violation for arbitrary lightlike or timelike geodesics starting at the origin.

The Gödel radius r_G can be identified [2] with the ro-

tation scalar

$$\Omega_G = \frac{\sqrt{2}c}{r_G}, \tag{2}$$

making it inversely proportional to the angular velocity of the rotating matter. Fig. 1 depicts several lightlike geodesics starting at the origin. Photons reach the Gödel radius, and their orbits are closed in the (xy)-subspace [33]. Thus r_G constitutes an optical horizon beyond which an observer located at the origin cannot see, because photons starting with $r_0 > r_G$ do not reach the origin. Due to the stationarity of Gödel's metric, there exists no gravitational redshift; only Doppler shift due to relative motion arises.

Comparable to asymptotic flat spacetimes, we can find an interpretation for this set of coordinates. Because the metric converges to the Minkowski metric of flat spacetime (in cylindrical coordinates) for $r \to 0$, we denote this set as the coordinates of an observer resting at the origin[34]. Coordinate time t and proper time τ of an observer at the origin are identical. Hence, if we want to make a statement on measurements performed by an observer, it is very convenient if he rests at the origin. Due to the homogeneity of Gödel's universe we can transform any physical situation in such a way that an arbitrary observer is then located at the new origin. The mathematical details are provided in Sec. IV.

We denote an observer resting at the origin by **O**, other resting observers by $\mathbf{A}, \mathbf{B}, \mathbf{C}$ and traveling observers (or photons) by **T**. Fig. 2 illustrates a possible CTC. A traveler **T** starts at the origin, accelerates beyond the horizon, travels along a circular PTC into the past, reenters the horizon, and then reaches the origin at the same coordinate time of departure. The resulting curve is a non-circular CTC. Time travel is only possible beyond the horizon, because light cones intersect the plane of constant coordinate time for all $r > r_G$. Hence, a traveler can travel into his own future but into the past of the observer **O**.

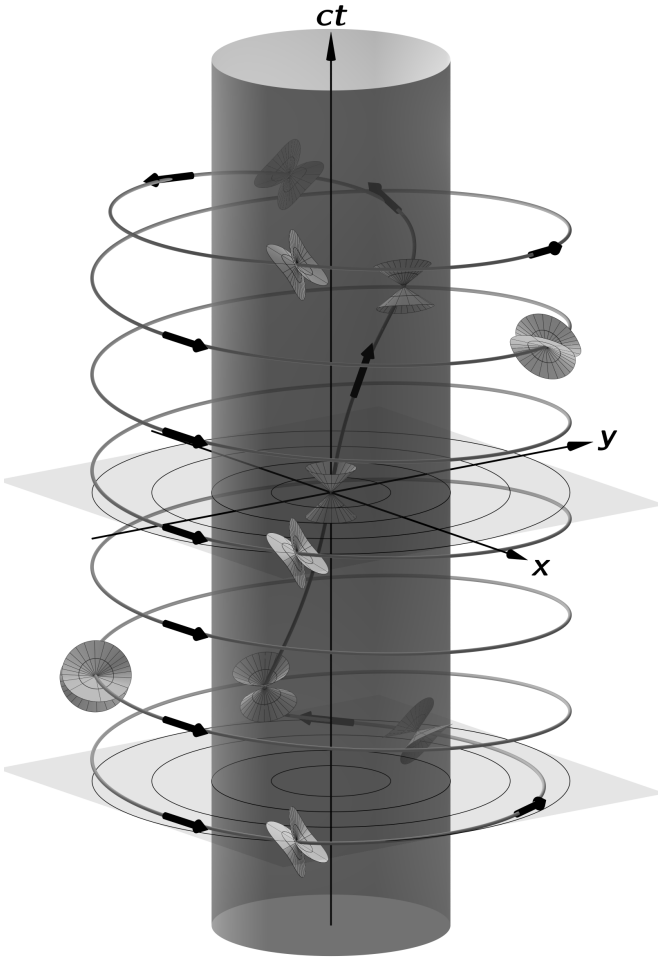

FIG. 2: Chronological structure of Gödel's universe. In this xyt-diagram a possible timelike worldline is depicted. A traveler **T** could move on this curve, propagating in his own local future at any given point. Beyond the horizon (gray cylinder) he travels into the past of an observer located at the origin. The worldline itself is a CTC, because the traveler departs from and returns to the origin at the same coordinate time t. For an observer at the origin, coordinate time and proper time coincide. The figure illustrates Gödel's original idea to prove that there exist CTCs through every point in spacetime [1].

B. Equations of motion

The geodesic equations

$$\ddot{x}^\mu + \Gamma^\mu_{\rho\sigma}\dot{x}^\rho\dot{x}^\sigma = 0 \tag{3}$$

govern the propagation of light or freely moving particles. In this section, any derivative is with respect to an affine parameter λ (for lightlike geodesics) or with regard to proper time τ (for timelike motion). Because these equations are of second order in λ or τ, respectively, initial conditions for position and direction have to be specified. If a massive particle is moving on an arbitrary timelike worldline $x^\mu(\tau)$, a four-acceleration

$$a^\mu = \ddot{x}^\mu + \Gamma^\mu_{\rho\sigma}\dot{x}^\rho\dot{x}^\sigma, \tag{4}$$

must act on the particle. An arbitrary vector X along this worldline (with tangent u^μ) will be Fermi-Walker transported according to

$$\begin{aligned} 0 =& \frac{dX^\beta}{d\tau} + X^\gamma u^\alpha \Gamma^\beta_{\alpha\gamma} + \\ & \frac{1}{c^2}\left(g_{\gamma\sigma}u^\sigma a^\beta - g_{\gamma\sigma}a^\sigma u^\beta\right) X^\gamma. \end{aligned} \tag{5a}$$

A vector on a geodesic will be parallel-transported using $a^\mu = 0$ in the equations above.

To derive the equations of geodesical motion we here use the Lagrangian formalism. The Lagrangian $\mathcal{L} =$

$g_{\mu\nu}u^\mu u^\nu$ for Gödel's metric (1) reads

$$\begin{aligned}\mathcal{L} &= -c^2\dot{t}^2 + \frac{\dot{r}^2}{1+(r/r_G)^2} + r^2\left[1+(r/r_G)^2\right]\dot{\varphi}^2 \\ &\quad +\dot{z}^2 - \frac{2\sqrt{2}r^2c}{r_G}\dot{t}\dot{\varphi}. \end{aligned} \tag{6}$$

Additionally, the constraint $\mathcal{L} = g_{\mu\nu}u^\mu u^\nu = \kappa c^2$ has to be fulfilled. The type of a geodesic is determined by the parameter κ. For timelike geodesics we have $\kappa = -1$, whereas lightlike geodesics require $\kappa = 0$.

Using the Euler-Lagrange equations of motion one finds three constants of motion $k_i = \partial\mathcal{L}/\partial\dot{x}^i$, where

$$k_0 = -c\dot{t} - \frac{\sqrt{2}r^2}{r_G}\dot{\varphi}, \tag{7a}$$

$$k_2 = r^2\left[1-(r/r_G)^2\right]\dot{\varphi} - \frac{\sqrt{2}r^2c}{r_G}\dot{t}, \tag{7b}$$

$$k_3 = \dot{z}. \tag{7c}$$

The quantities k_0, k_2 and k_3 represent the conservation of energy, angular momentum, and z-component of momentum, respectively. These three constants can be solved for $\dot{t}, \dot{\varphi}$ and $\dot{z}$. Substituting the result of this calculation in eq. (6), the Lagrangian becomes solely dependent on r and $\dot{r}$. Using the constraint $\mathcal{L}(r,\dot{r}) = \kappa c^2$ we can solve this equation for $\dot{r}$. We then obtain the equations of motion for both photons and massive particles in the form

$$c\dot{t} = -k_0\frac{1-(r/r_G)^2}{1+(r/r_G)^2} - \frac{\sqrt{2}k_2}{r_G\left[1+(r/r_G)^2\right]}, \tag{8a}$$

$$\begin{aligned}\dot{r}^2 &= (\kappa c^2 - k_3^2)\left[1+(r/r_G)^2\right] - \frac{k_2^2}{r^2} + \\ &\quad \frac{2\sqrt{2}k_0k_2}{r_G} + k_0^2\left[1-(r/r_G)^2\right], \end{aligned} \tag{8b}$$

$$\dot{\varphi} = \frac{k_2 - \sqrt{2}r^2k_0/r_G}{r^2\left[1+(r/r_G)^2\right]}, \tag{8c}$$

$$\dot{z} = k_3. \tag{8d}$$

C. Initial conditions

Now, we will formulate the initial conditions of arbitrary geodesics using the constants of motion. These initial conditions will be expressed with respect to a local frame of reference, because this formulation facilitates statements on measurements done by arbitrary observers.

1. Local frame of reference

Any vector $\mathbf{u}$ can be expressed with respect to a particular coordinate system or a local frame of reference $\{\mathbf{e}_{(a)} : a = 0,1,2,3\}$, i. e.

$$\mathbf{u} = u^\mu\partial_\mu = u^{(a)}\mathbf{e}_{(a)}. \tag{9}$$

Greek indices denote vectors in coordinate representation, whereas Latin indices in round brackets are used for vectors expressed in a local frame. To obtain an orthonormal system the condition

$$\mathbf{g}(\mathbf{e}_{(a)},\mathbf{e}_{(b)}) := g_{\mu\nu}\mathbf{e}^\mu_{(a)}\mathbf{e}^\nu_{(b)} = \eta_{(a)(b)}, \tag{10a}$$

$$\eta_{(a)(b)} = \mathrm{diag}(-1,1,1,1), \tag{10b}$$

has to be fulfilled, where the transformation matrices satisfy

$$\mathbf{e}^\mu_{(a)}\mathbf{e}^{(a)}_\nu = \delta^\mu_\nu. \tag{11}$$

We choose the local frame of reference of a static observer – comoving with the rotating matter and resting with respect to the cylindrical set of coordinates – and find that

$$\mathbf{e}_{(0)} = \frac{1}{c}\partial_t, \tag{12a}$$

$$\mathbf{e}_{(1)} = \sqrt{1+(r/r_G)^2}\partial_r, \tag{12b}$$

$$\mathbf{e}_{(2)} = \frac{1}{r\sqrt{1+(r/r_G)^2}}\left(-\frac{\sqrt{2}r^2}{r_Gc}\partial_t + \partial_\varphi\right), \tag{12c}$$

$$\mathbf{e}_{(3)} = \partial_z. \tag{12d}$$

This tetrad, however, is not well-defined for $r = 0$. Because the angular coordinate is undefined at $r = 0$, we cannot formulate initial directions in ∂_φ-direction. Nevertheless we can exploit the rotational symmetry of this spacetime. A geodesic can start with $u_0^\varphi = 0$ and then be rotated around the z-axis afterwards to generate geodesics starting at the origin and propagating in arbitrary initial direction. Another possibility is to transform the tetrad as well as the line element itself to Cartesian coordinates to avoid the coordinate singularity in $r = 0$. Unfortunately, Gödel's universe loses its mathematical elegance when considering a set of coordinates which is not adjusted to the symmetries of the spacetime.

2. Local formulation of the constants of motion

We can express the constants of motion, eq. (7), with respect to the chosen local frame of reference, eq. (12). The result for both lightlike and timelike geodesics is

$$k_0 = -u_0^{(0)}, \tag{13a}$$

$$k_2 = r_0\sqrt{1+(r_0/r_G)^2}u_0^{(2)} - \frac{\sqrt{2}r_0^2}{r_G}u_0^{(0)}, \tag{13b}$$

$$k_3 = u_0^{(3)}. \tag{13c}$$

The parameter $r_0 = r(0)$ is the initial radial coordinate of the geodesic. Because any vector $\mathbf{u} = u^{(a)}\mathbf{e}_{(a)}$ expressed in a local system is treated like any vector in special relativity, the sign of $u_0^{(0)}$ determines whether the geodesic is evolving into the future (+) or into the past (−). Hence, k_0 is associated with the time direction.

D. Killing vectors

Solving the Killing equations $\xi_{\mu;\nu}+\xi_{\nu;\mu}=0$ for Gödel's universe yields five Killing vector fields (cf. [2]), which read

$$\xi_0^\mu = \begin{pmatrix}1\\0\\0\\0\end{pmatrix}, \quad \xi_2^\mu = \begin{pmatrix}0\\0\\1\\0\end{pmatrix}, \quad \xi_3^\mu = \begin{pmatrix}0\\0\\0\\1\end{pmatrix}, \tag{14a}$$

$$\xi_1^\mu = \frac{1}{q(r)}\begin{pmatrix}\frac{r}{\sqrt{2}c}\cos\varphi\\ \frac{r_G}{2}\left[1+(r/r_G)^2\right]\sin\varphi\\ \frac{r_G}{2r}\left[1+2(r/r_G)^2\right]\cos\varphi\\ 0\end{pmatrix}, \tag{14b}$$

$$\xi_4^\mu = \frac{1}{q(r)}\begin{pmatrix}\frac{r}{\sqrt{2}c}\sin\varphi\\ -\frac{r_G}{2}\left[1+(r/r_G)^2\right]\cos\varphi\\ \frac{r_G}{2r}\left[1+2(r/r_G)^2\right]\sin\varphi\\ 0\end{pmatrix}, \tag{14c}$$

where

$$q(r)=\sqrt{1+(r/r_G)^2}. \tag{15}$$

The first three Killing vectors (eq. (14a)) are trivial, corresponding to the constants of motion (13), and represent infinitesimal transformations in t, φ and z, respectively. Eqns. (14b) and (14c) reveal that a radial transformation generally affects time and angular coordinate as well. Note that lower indices in Killing vectors serve to distinguish different vector fields.

Taking advantage of the Killing vectors (14), the generators of the corresponding Lie algebra read $X_k = \xi_k^\alpha \partial/(\partial x^\alpha)$. In this representation the structure constants C_{ijk} follow from the Lie brackets $[X_i, X_j] = C_{ijk}X_k$ according to

$$[X_1,X_2] = -[X_2,X_1] = -X_4, \tag{16a}$$
$$[X_2,X_4] = -[X_4,X_2] = -X_1, \tag{16b}$$
$$[X_1,X_4] = -[X_4,X_1] = \frac{1}{\Omega_G}X_0 + X_2, \tag{16c}$$
$$\tag{16d}$$

where $[X_i,X_j] = X_iX_j - X_jX_i$.

It is worthwhile noting that the set of generators defined by $L_1 = X_4$, $L_2 = X_1$, $L_3 = -i(X_2 + X_0/\Omega_G)$ satisfies the angular momentum algebra $[L_i,L_j] = i\varepsilon_{ijk}L_k$, as shown by Figuareido [24]. Here $i,j,k \in \{1,2,3\}$ and ε_{ijk} represents the three-dimensional Levi-Cevita symbol. Moreover, the remaining generators $L_0 = X_0$ and $L_4 = X_3$ commute with L_1, L_2 and L_3. This feature is used e. g. in the analysis of the scalar wave equation in Gödel's Universe [24, 25].

III. SOLUTION TO THE GEODESIC EQUATIONS

A. Geodesics for special initial conditions

In this section, we will present the solution of the geodesic equations for special initial conditions. We consider arbitrary timelike and lightlike geodesics starting at the origin of the coordinate system. Lightlike geodesics alone had been considered by Kajari et. al. [2]. Although the general solution to the geodesic equations is introduced in the next section, the special solution is necessary to overcome the coordinate singularity in $r = 0$. In principle, we could obtain the special solution from the general solution by applying the limit $r_0 \to 0$ for the initial radial coordinate r_0. Unfortunately, this limit is complicated to calculate.

The constants of motion, eq. (13), simplify for geodesics starting at the origin. In particular, k_2 vanishes, and the equations of motion now read

$$c\dot{t} = -k_0\frac{1-(r/r_G)^2}{1+(r/r_G)^2}, \tag{17a}$$
$$\dot{r}^2 = K_+ - K_-(r/r_G)^2, \tag{17b}$$
$$\dot{\varphi} = \frac{-\sqrt{2}k_0}{r_G\left[1+(r/r_G)^2\right]}, \tag{17c}$$
$$\dot{z} = k_3, \tag{17d}$$

using the abbreviations

$$K_+ = \kappa c^2 + k_0^2 - k_3^2, \tag{18a}$$
$$K_- = -\kappa c^2 + k_0^2 + k_3^2. \tag{18b}$$

Solving these equations is straightforward and outlined in Sec. A 1 a. The solution reads

$$t(\lambda) = \frac{k_0}{c}\lambda + \frac{\sqrt{2}r_G}{c}\left[\varphi_1(\lambda)+p_{1/2}(\lambda)\right]+t_0, \tag{19a}$$
$$r(\lambda) = r_G\sqrt{\frac{K_+}{K_-}}\left|\sin\left(\sqrt{B_1}\lambda\right)\right|, \tag{19b}$$
$$\varphi(\lambda) = \varphi_1(\lambda)+p_{1/2}(\lambda)-p_0(\lambda)+\varphi_0, \tag{19c}$$
$$z(\lambda) = k_3\lambda, \tag{19d}$$

with

$$p_q(\lambda) = \pi\sigma_0\left\lfloor\frac{\sqrt{B_1}}{\pi}\lambda+q\right\rfloor, \tag{20a}$$
$$\varphi_1(\lambda) = \arctan\left(\frac{k_0\sqrt{2}}{\sqrt{K_-}}\tan\left(-\sqrt{B_1}\lambda\right)\right), \tag{20b}$$

where we used the constant B_1 from eq. (21a) and the abbreviation for the initial temporal direction σ_0 (cf. eq. (22a)). The expression $\lfloor y\rfloor$ is the mathematical floor function, which ensures the continuous differentiability of the solution, except for $r = 0$. As stated at the end of

Sec. II C 1, we cannot directly generate geodesics starting in the ∂_φ-direction due to the coordinate singularity of the cylindrical coordinate system. This coordinate singularity is avoided by interpreting the integration constant φ_0 as the local starting direction in the (xy)-plane. For $\varphi_0 = 0$, the geodesic starts in positive x-direction if the particle propagates into the future, i. e. $k_0 < 0$. On the other hand $\varphi_0 = \pi/2$ results in a geodesic starting in negative y-direction for $k_0 > 0$. Note that the special solution of the geodesic equations, eqns. 19, generalize the results of the work of Kajari et. al. [2]. Setting $k_3 = 0$ and $\kappa = 0$ reproduces their results regarding lightlike motion in the (xy)-subspace.

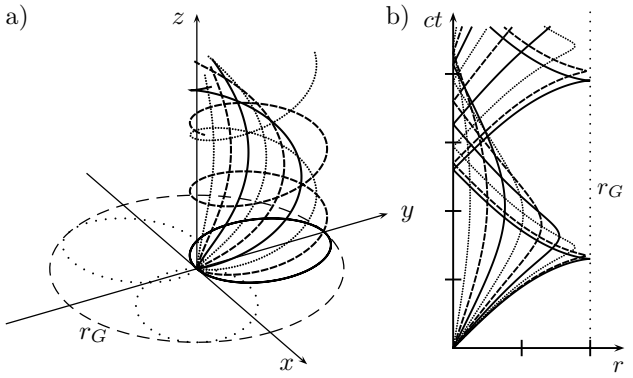

FIG. 3: Lightlike geodesics starting at the origin. For better orientation, the Gödel horizon and three planar geodesics (compare Fig. 1) are provided in Fig. 3a. The non-planar geodesics are solid, dashed or densely dotted curves. The angle between neighboring geodesics is 10°. Fig. 3b: Radial coordinate as a function of coordinate time. Non-planar geodesics do not reach the Gödel radius. Timelike geodesics are of similar shape but reach smaller maximal radial distances from the origin.

Fig. 3 depicts several geodesics with non-zero initial velocity in $\mathbf{e}_{(3)}$-direction. Those geodesics do not reach the Gödel horizon. However, the optical Gödel horizon is of cylindrical shape, because geodesics with $u^{(3)} = \epsilon$ with $\epsilon \ll 1$ (almost planar geodesics) come arbitrarily close to the horizon for sufficiently small ϵ. These geodesics still reach any z-value after an appropriate number of cycles. Timelike geodesics also do not reach the horizon when starting from the origin, even in the planar case. Both effects are caused by the radial solution, eq. (17b), where the prefactor becomes $\sqrt{K_+/K_-} < 1$. Fig. 3b shows that geodesics starting at the origin do not violate causality – with respect to the observer $\mathbf{O}$ – because $dt/d\lambda \geq 0$.

B. Geodesics for arbitrary initial conditions

We will now discuss the general solution to the geodesic equations for timelike and lightlike motion. For this task, the full geodesic equations (8) for arbitrary initial conditions, eqns. (13), have to be solved. An outline of the derivation is provided in Sec. A 1 b. We use the abbreviations

$$B_1 = \frac{K_-}{r_G^2}, \quad B_2 = -\frac{k_2^2}{r_G^4}, \quad B_3 = \frac{K_+}{r_G^2} + \frac{2\sqrt{2}k_0k_2}{r_G^3}, \tag{21a}$$

$$B_4 = \sqrt{(r_G/2)^2K_+^2 + K_+(\sqrt{2}r_Gk_0k_2 + k_2^2)}, \tag{21b}$$

$$C_1 = \frac{1}{2\sqrt{B_1}} \arcsin\left(\frac{r_G^4B_3 - 2r_0^2K_-}{2r_GB_4}\right), \tag{21c}$$

where the constants K_+ and K_- are identical to those defined in eqns. (18). To distinguish radially outgoing or incoming initial conditions as well as the initial temporal direction of a geodesic, we use the signum functions

$$\sigma_0 = \mathrm{sgn}(u_0^{(0)}), \tag{22a}$$

$$\sigma_1 = \mathrm{sgn}(u_1^{(0)}). \tag{22b}$$

The integration constant C_1 of the radial equation (8b) is determined via $r(0) = r_0$. Furthermore, we introduce the auxiliary functions

$$v(\lambda) = \sqrt{B_1}(-\sigma_1\lambda + C_1), \tag{23a}$$

$$\varphi_2(\lambda) = \arctan\left\{\frac{\sigma_1 r_G^2}{2\sqrt{B_1}(k_2 + \sqrt{2}r_Gk_0)} \times \left[(2B_1 + B_3)\tan(v(\lambda)) - \sqrt{B_3^2 + 4B_1B_2}\right]\right\}, \tag{23b}$$

$$\varphi_3(\lambda) = \arctan\left\{\frac{\sigma_1 r_G^2}{2\sqrt{B_1}k_2} \times \left[B_3\tan(v(\lambda)) - \sqrt{B_3^2 + 4B_1B_2}\right]\right\}, \tag{23c}$$

$$\tilde{p}(\lambda) = \pi\sigma_1\sigma_0\left[\frac{\sqrt{B_1}}{\pi}(\sigma_1\lambda - C_1) + \frac{1}{2}\right], \tag{23d}$$

where the function $\tilde{p}(\lambda)$ ensures the continuous differentiability of the solution and is analogous to eq. (20a) of the special solution. Finally, the analytical solutions for both arbitrary timelike and lightlike geodesics are found in the form

$$t(\lambda) = \frac{k_0}{c}\lambda + \frac{\sqrt{2}r_G}{c}\left[\varphi_2(\lambda) + \tilde{p}(\lambda)\right] + C_3, \tag{24a}$$

$$r(\lambda) = r_G\sqrt{\frac{r_G^3B_3/2 - B_4\sin(2v(\lambda))}{r_GK_-}}, \tag{24b}$$

$$\varphi(\lambda) = \varphi_2(\lambda) - \varphi_3(\lambda) + C_2, \tag{24c}$$

$$z(\lambda) = k_3\lambda + z_0. \tag{24d}$$

The integration constants C_2 and C_3 can be specified by $\varphi(0) = \varphi_0$ and $t(0) = t_0$. If the geodesic is only directed along the local $\mathbf{e}_{(3)}$-axis, i. e. $u_0^{(1)} = u_0^{(2)} \equiv 0$, we

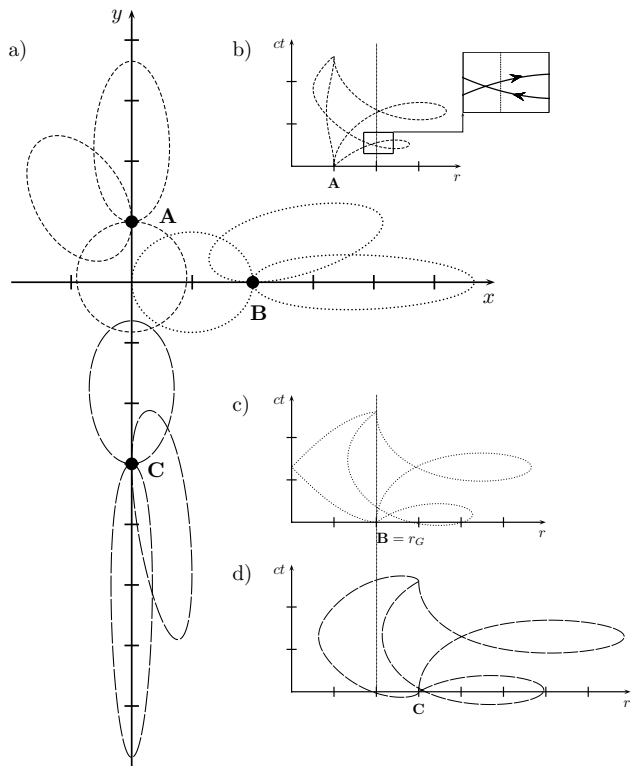

FIG. 4: Planar lightlike geodesics resulting from the general analytical solution to the geodesic equations. In Fig. 4a, nine geodesics at different initial positions are shown. Position **A** is at $r_0 = r_G/2$, position **B** shows geodesics starting on the horizon r_G, and in **C** we have $r_0 = 3r_G/2$. At each starting point geodesics propagate in $+\mathbf{e}_{(1)}$- or $\pm\mathbf{e}_{(2)}$-direction, respectively. Non-planar geodesics show a behavior similar to the special solution, Fig. 3, i. e. are smaller in radial extent. Figs. 4b-d show the radial coordinate of the geodesics as a function of coordinate time.

obtain straight lines parallel to the z-axis, where $t(\lambda) = k_0\lambda/c + t_0$.

In Fig. 4, several planar lightlike geodesics are depicted. Fig. 4a shows the projection onto the (xy)-subspace and Fig. 4b-d display the correlation between radial coordinate and coordinate time t. Most photons in Fig. 4 partially travel back through time. This travel through time is in most cases restricted to regions beyond the Gödel horizon and therefore not measurable by the observer **O**. Fig. 4b, in which several geodesics starting at $r_0 = r_G/2$ are depicted, reveals an exception. The magnified square shows that the corresponding photon reenters the Gödel horizon before crossing it.

To investigate how far a traveler **T** can travel into the past of an observer **O**, we use the general solution to the geodesic equations (24). We consider an arbitrary initial position and any initial direction within the local $\{\mathbf{e}_{(1)}, \mathbf{e}_{(2)}\}$-subspace. It can be shown that $u_0^{(3)}$ must be zero to maximize time travel [35]. Solving the radial solution, eq. (24b), with respect to the curve parameter results in an infinite number of solutions due to the periodicity of $r(\lambda)$. We choose the first two solutions λ_1 (where the photon or massive particle arrives at the horizon) and λ_2 (where it reappears from beyond the horizon). Inserting λ_1 and λ_2 into the time solution, eq. (24a), yields a difference in coordinate time

$$\Delta t = t(\lambda_2) - t(\lambda_1). \tag{25}$$

Again, coordinate time and proper time of an observer **O** are identical. Fig. 5 shows the result of these considerations. In Fig. 5a, the minimal time difference Δt, eq. (25), is depicted for a given initial radial coordinate r_0. We find these values by numerically searching the angle ξ_0 for fixed r_0, where Δt becomes minimal. The local angle between the starting direction and the $\mathbf{e}_{(1)}$-axis is denoted as ξ_0. The correlation between ξ_0 and r_0 is shown in Fig. 5b. Radii $\rho_1, \ldots, \rho_5$ denote certain initial positions for the lightlike case, which we will now discuss. We set $\rho_1 = r_G/4$, $\rho_2 = r_G/2$, $\rho_3 = r_G$, $\rho_4 \approx 1.4r_G$, and $\rho_5 \approx 1.7r_G$. Obviously, time travel is only possible for $r_0 \lesssim \rho_5$.

Fig. 5a reveals that there exists a maximum time travel (i. e. minimal Δt with $\Delta t < 0$) for a given initial velocity. In the time travel region ($0 \leq r_0 \leq \rho_5$ in the lightlike case), Δt appears constant for a large region of initial radii ($\rho_1 \leq r_0 \leq \rho_4$). Unfortunately, equation (25) is too complicated to treat it analytically despite its simple structure. Analytical investigations are restricted to special cases, and for a detailed analysis in general we have to resort to numerical investigations. We find that Δt is constant up to at least within 10^{-10} in the region $\rho_1 \leq r_0 \leq \rho_4$. The global minimum can be estimated with $\Delta t(r_0 = \rho_2, \xi_0)$, because $(d\Delta t(r_0 = \rho_2, \xi_0))/(d\xi_0) \equiv 0$ (exactly) for $\xi_0 = 0$. The global minimum $\Delta T^c_{\min} = \Delta t(r_0 = \rho_2, \xi_0)$ then reads

$$\begin{aligned} \Delta T^c_{\min} &= \frac{r_G}{2c}\left[\pi(\sqrt{2}-1) - 2\sqrt{2}\arctan\left(\frac{\sqrt{7}}{5}\right)\right] \\ &= -\frac{r_G}{c} \times 3.7645439 \times 10^{-2}. \end{aligned} \tag{26}$$

For timelike geodesical motion, the plateau region becomes smaller but is still constant up to at least within 10^{-10}. The maximum time travel on timelike geodesics $\Delta T_{\min}(v) < \Delta T^c_{\min}$, converges to $\Delta T^c_{\min}$ for $v \to c$, and scales with r_G exactly as in the lightlike case. A traveler **T** needs a velocity of at least $v = v_{\min} \gtrsim 0.980172c$ (with respect to the local frame (12)) to travel through time. If v is smaller, $\Delta T_{\min}(v)$ is defined but positive. In this case, the massive particle might travel through time, but only beyond the horizon and, thus, not visible to the observer **O**.

Fig. 5b shows the correlation between a certain initial radial coordinate r_0 and the local angle ξ_0 under which the geodesic has to start for maximum time travel. In the region $\rho_1 \leq r_0 \leq \rho_4$ there exist two initial directions ξ_0 under which the time difference $\Delta T^c_{\min}$ is found. Apart

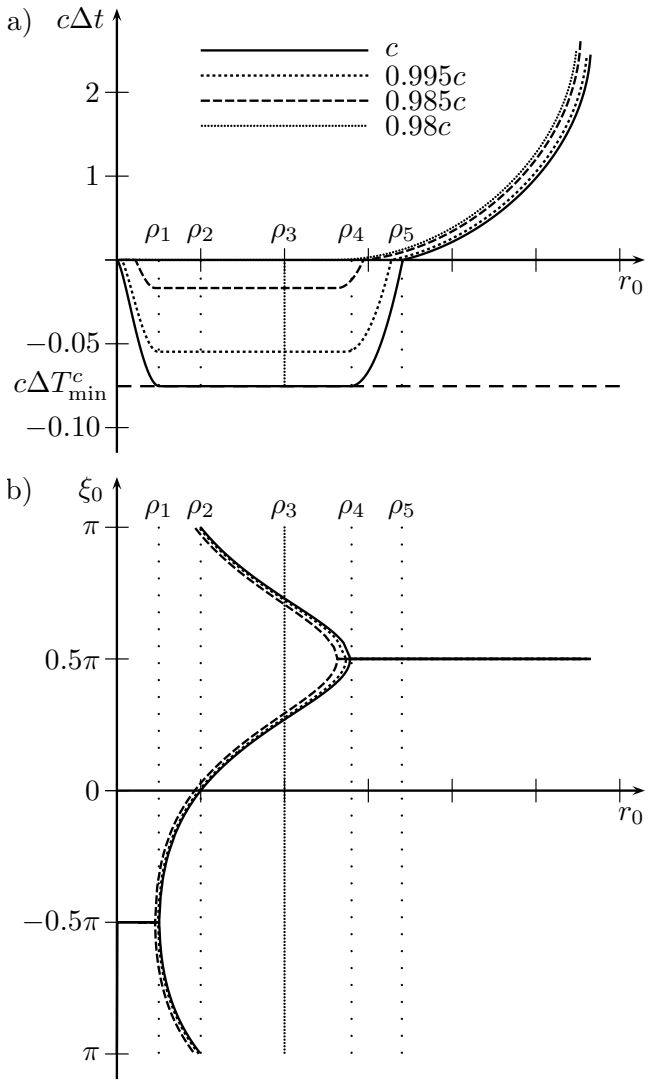

FIG. 5: Time travel on geodesics. Fig. 5a shows how far a traveler **T** (photon or massive particle) can travel into the past for a given initial radial coordinate r_0 (maximum time travel $\Delta t_{\min}$ for fixed r_0). Fig. 5b explains under which direction the traveling particle has to start, where ξ_0 denotes the angle to the local $\mathbf{e}_{(1)}$-axis in the $\{\mathbf{e}_{(1)}, \mathbf{e}_{(2)}\}$-subspace. Starting in another direction can also result in time travel, but results in $\Delta t > \Delta T_{\min}$. Note that the time axis in Fig. 5a is magnified by a factor of 20 for $\Delta t < 0$.

from this region, ξ_0 is unique for a given r_0 and either takes the value $\pi/2$ or $-\pi/2$. For radii $r_0 > \rho_4$, the initial direction is parallel to the $\mathbf{e}_{(2)}$-axis of the local rest frame (eqns. (12)). Hence, the geodesic starts locally parallel to the motion of matter. For $r < \rho_1$, it starts into the opposite direction.

To investigate if causality is violated, we detail the results of [20]. The situation now discussed is depicted in Fig. 6 and Fig. 7 from two different perspectives. In Fig. 6, we see a radially outgoing lightlike geodesic starting at $r_0 = r_G/2$. For this geodesic, we achieve the maximum time travel, cf. eq. (26).

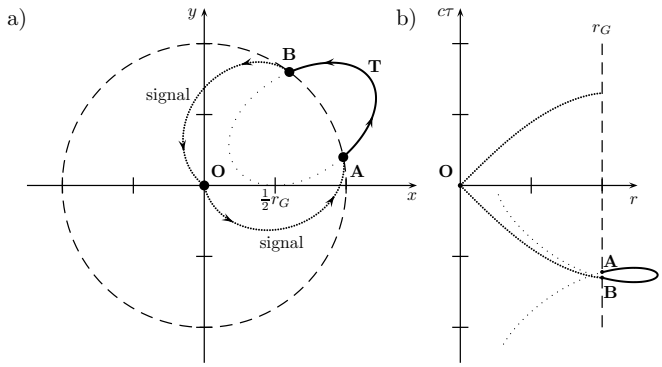

FIG. 6: Testing if causality can be violated on geodesics. A traveler **T** moves partially beyond the horizon of an observer **O** (Fig. 6a). He leaves the horizon passing observer **A** and reenters it passing **B**. The observer **B** sends a light pulse to **O**, informing him on the arrival of **T**. Then, **O** signals **A** this information. If this information arrived *before* **T** passes the horizon, **B** could stop the traveler, resulting in a paradox. Fig. 6b reveals that no causality violation arises, because the information arrives in the future light cone of the event "**T** passes **A**". Note that we use a lightlike geodesic for the path of **T** as the limiting case $v \to c$.

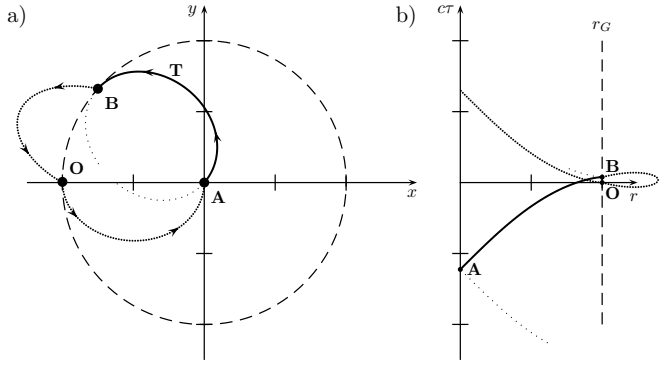

FIG. 7: Isometrically transporting **A** to the spatial origin yields the situation from the point of view of observer **A** (Fig. 7a). Both observers **O** and **B** are located on the horizon of **A**. The traveler's movement is restricted to the interior of *this* horizon and no time travel arises. From this perspective, the signal from **B** to **O** travels back in time with respect to **A** (Fig. 7b).

Consider an observer **T**, traveling extremely close to the speed of light. Then, the traveler's path is almost identical to the lightlike geodesic depicted in Fig. 6. An observer **O** will see a traveler **T** only on those segments of the geodesic that are within the observer's horizon. Fig. 4b reveals that, from **O**'s perspective, **T** reenters from beyond the horizon (**B**) before leaving it (**A**). Due to the finite speed of light, the observer will not see the traveler at the moment he reenters or leaves the horizon but a certain light travel time later. Because the Gödel horizon is of circular shape, the time span that the light

takes to travel from the horizon to the origin is independent of the exact position on the horizon (as long as we restrict ourselves to the (xy)-plane). Therefore, this time span is identical for the traveler reentering the horizon as well as leaving it. We can, as a consequence, neglect the light travel time in our current considerations. Hence, the observer **O** will see **T** time travel on a geodesical path and this effect is not a mere consequence of the finiteness of the speed of light. Now, we will discuss whether or not this time travel violates causality.

The relevant geodesics segment of **T** beyond the horizon of the geodesic is not a CTC, because the particle crosses the horizon at different angular coordinates and the path is therefore not closed. Although the cause and the effect – **T** must leave the horizon before reentering it – appear reversed, we do not have a causality violation in the classical meaning. A violation of causality would only arise, if the effect (information about the reentered traveler) could be transported to the local past light cone of the cause (event of the traveler leaving the horizon). In other words: The observer **O** had to provide the information about the time travel (from his point of view) to **A** *before* **T** crosses the horizon in the "first" place. Therefore, the observer **B** has to signal **O** the arrival of the traveler and **O** then has to send this information to **A**. Finally, **A** had to receive this signal *before* the traveler passes his position. Only then he could decide to stop the traveler and we ended in a paradox situation, where causality was violated.

Although a lightlike geodesic is depicted, we can still use this image as the limiting case $v \to c$. It can be easily estimated, using $\lambda = \pi/(2\sqrt{B_1})$ in eq. (19a), that a signal from the origin to the horizon would need a time span (measured by **O**) of

$$\Delta\tau = \frac{\pi r_G}{c}\left(\frac{\sqrt{2}-1}{2}\right) \approx \frac{r_g}{c} \times 1.30129. \tag{27}$$

Signaling back and forth doubles this time span. It is by far longer than the absolute value of the maximum time travel, eq (26). The signal of the reentering traveler therefore reaches the observer **A** in the future light cone of the event of **T** crossing the horizon, cf. Fig. 6b. Therefore, although the traveler travels partially back in time, causality is conserved.

From the perspectives of the observers **A** and **B** the traveler behaves causally normal, because their positions are both located on the same geodesic and, therefore, this geodesic is restricted entirely to the respective horizon of each observer. In Fig. 7, the experiment is shown with respect to **A**. An isometric transport of the observer **B** to the origin yielded an equivalent characterization of the situation. Both observers will consequently see the traveler at all times and the traveler will never move back in time. However, one of the signals from or to **O** will now partially travel back in time with respect to the observer now resting at the origin. Therefore, for each of the three observers exactly one segment of the three geodesics – the traveler's path or one of the geodesics transporting signals – describes a travel back through time. Because we regard the limit $v \to c$ for the traveler's velocity, each travel through time (for the respective observer) is equal to the maximum time travel on geodesics, eq. (26).

In any case, the traveler **T** will not travel through time with respect to his *own* rest frame. His proper time τ evolves unaffected from the considerations and measurements done by the observer **O**. Due to the homogeneity of the spacetime, the traveler T always rests at the center of "his" Gödel horizon.

IV. FINITE ISOMETRIC TRANSFORMATIONS

In this section, we derive analytical expressions for finite isometric transformations for all five Killing vector fields of Gödel's universe.

A. Finite transformation of points

A Killing vector ξ^μ is defined [26] as an infinitesimal displacement

$$x'^\mu = x^\mu + \varepsilon\,\xi^\mu(x^\nu), \quad \varepsilon \ll 1, \tag{28}$$

which leaves the metric unchanged. When we restrict ourselves to a one-parameter family of transformations with $x'^\mu = x^\mu(\eta + \varepsilon)$ and $x^\mu = x^\mu(\eta)$, the previous relation is equivalent to the following system of first order differential equations

$$\frac{dx^\mu(\eta)}{d\eta} = \xi^\mu\left(x^\nu(\eta)\right) . \tag{29}$$

Together with the initial condition x_0^μ, they uniquely determine the orbits of the corresponding Killing vector field [27]. The solutions of these equations are lines of finite isometric displacements, shown in Fig. 8 and Fig. 9 for the Killing vector field ξ_1^μ of the Gödel metric.

While the solution for the trivial Killing vector fields, eq. (14a), is obvious and describes mere straight lines along t, φ and z in cylindrical coordinates, the solution to eqns. (14b) and (14c) is more difficult to obtain. We discuss the derivation of the solution in Sec. A 2 a. The complete solution to the equations of isometric transport (29) for the Killing vector field ξ_1^μ (eq. (14b)) and

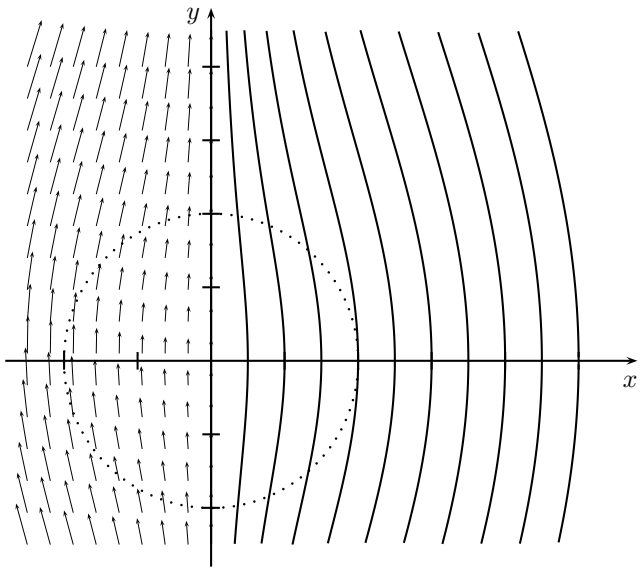

FIG. 8: Projection of Killing vector field ξ_1^μ onto the xy-plane (t =const. and z = const. in Cartesian coordinates). The left half-plane shows the vector field itself, and the right half-plane depicts the integral curves of finite isometric displacements along ξ_1^μ. The Gödel horizon appears as the dotted circle.

ξ_4^μ (eq. (14c)) reads

$$t_1(\eta) = \sigma\frac{\sqrt{2}r_G}{c}\arctan\left(\frac{D_2e^\eta + (r_G/2)^2}{\sqrt{D_1D_2-(r_G/2)^4}}\right) + D_3, \tag{30a}$$

$$r_1(\eta) = \sqrt{D_1e^{-\eta} + D_2e^\eta - r_G^2/2}, \tag{30b}$$

$$\varphi_1(\eta) = \sigma\arcsin\left(\frac{-D_1e^{-\eta}+D_2e^\eta}{r_1(\eta)\sqrt{r_1^2(\eta)+r_G^2}}\right) + \frac{1-\sigma}{2}\pi, \tag{30c}$$

$$z_1(\eta) = D_4, \tag{30d}$$

and

$$t_4(\eta) = t_1(\eta), \quad r_4(\eta) = r_1(\eta), \quad z_4(\eta) = z_1(\eta), \tag{31a}$$

$$\varphi_4(\eta) = \varphi_1(\eta) + \pi/2. \tag{31b}$$

The lower indices in the solution denote the connection to the Killing vectors ξ_1 and ξ_4, respectively. The parameter σ distinguishes whether the starting angle φ_0 is within the right or the left half plane and reads

$$\sigma = \begin{cases} +1, & \text{if } \varphi_0 \in \text{right half plane,} \\ -1, & \text{if } \varphi_0 \in \text{left half plane.} \end{cases} \tag{32}$$

If the starting angle φ_0 is $\pm\pi/2$, i. e. the starting point is on the y-axis, $t_i(\eta)$ and $\varphi_i(\eta)$ become constant. Now, we set the integration constants to

$$D_1 = \frac{1}{2}\left(r_0^2 + r_G^2/2 - r_0\sqrt{r_0^2+r_G^2}\sin\varphi_0\right), \tag{33a}$$

$$D_2 = \frac{1}{2}\left(r_0^2 + r_G^2/2 + r_0\sqrt{r_0^2+r_G^2}\sin\varphi_0\right), \tag{33b}$$

$$D_3 = t_0 - \sigma\frac{\sqrt{2}r_G}{c}\arctan\left(\frac{D_2+(r_G/2)^2}{\sqrt{D_1D_2-(r_G/2)^4}}\right), \tag{33c}$$

$$D_4 = z_0, \tag{33d}$$

where r_0 and φ_0 are the initial radial coordinate and initial angle, respectively. The integration constants, eqns. (33), remain unaffected. This solution can easily be continuously continued to $r = 0$.

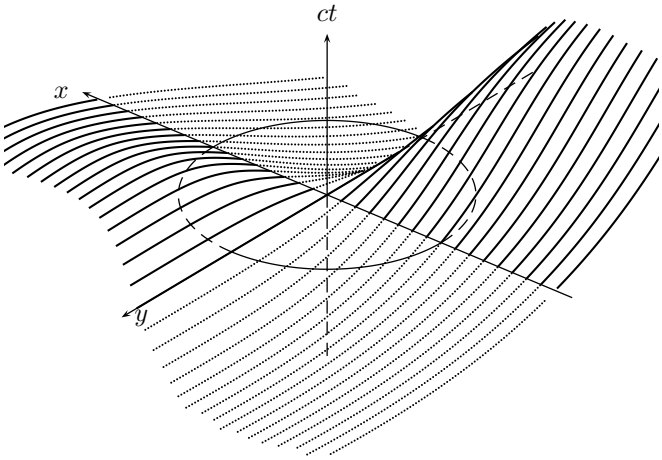

FIG. 9: Isometrically transporting points on the x-axis along the Killing vector field ξ_1^μ, showing the lines of finite isometric transport. Solid lines indicate transport to positive t-values, dotted lines illustrate negative time values. The Gödel radius appears as partially dashed circle.

B. Finite transformation of directions

So far we only know how to apply a finite isometric transformation to points in Gödel's universe. In order to transform geodesics we must find expressions for how to transform initial directions and local tetrads. This is equivalent to isometrically transporting a vector. Now we will form infinitesimal equations of isometric transport for vectors. The complete solutions to these equations of transport are presented in this section, their derivation is outlined in Sec. A 2 b.

Let $x^\mu(\lambda)$ be an arbitrary lightlike geodesic, timelike geodesic, or timelike worldline. The infinitesimal isometric transformation of this curve then reads

$$x'^\mu(\lambda) = x^\mu(\lambda) + \eta\xi^\mu\left(x^\nu(\lambda)\right). \tag{34}$$

Differentiation with respect to λ and setting $dx^\mu/d\lambda = u^\mu$ yields

$$\begin{aligned} u'^\mu(\lambda) &= u^\mu(\lambda) + \eta\frac{d}{d\lambda}\left[\xi^\mu\left(x^\nu(\lambda)\right)\right] \\ &= u^\mu(\lambda) + \eta\frac{d\xi^\mu}{dx^\nu}u^\mu(\lambda). \end{aligned} \tag{35}$$

Now we differentiate with respect to η. Because the resulting equation is valid for every λ, we omit the curve parameter, and without loss of generality arrive at

$$\frac{du^\mu}{d\eta} = \frac{d\xi^\mu}{dx^\nu}u^\nu. \tag{36}$$

The solution to this equation is an isometrically transported arbitrary vector along the lines of finite isometric displacements. For the trivial Killing vector fields (14a) we have $du^\mu/d\eta \equiv 0$, hence vectors remain unchanged when they are transported along these three fields. However, the situation of transport along the non-trivial vector fields, eqns. (14b) and (14c), is more interesting. The differential equations system for the Killing vector field (14b), using

$$\tilde{q}(r) = \sqrt{r_G^2 + r^2}, \tag{37}$$

reads

$$\frac{du^t}{d\eta} = \frac{r_G^3\cos\varphi}{\sqrt{2}cq^3(r)}\,u^r - \frac{rr_G\sin\varphi}{\sqrt{2}c\tilde{q}(r)}\,u^\varphi, \tag{38a}$$

$$\frac{du^r}{d\eta} = \frac{r\sin\varphi}{2\tilde{q}(r)}\,u^r + \frac{1}{2}\tilde{q}(r)\cos\varphi\,u^\varphi, \tag{38b}$$

$$\frac{du^\varphi}{d\eta} = -\frac{r_G^4\cos\varphi}{2r^2q^3(r)}\,u^r - \frac{(r_G^2/2 + r^2)\sin\varphi}{r\tilde{q}(r)}\,u^\varphi, \tag{38c}$$

$$\frac{du^z}{d\eta} = 0. \tag{38d}$$

As detailed in Sec. A 2 b, the solution with respect to the local tetrad (eqns. 12) is

$$u^{(0)}(\eta) = u_0^{(0)}, \tag{39a}$$

$$u^{(1)}(\eta) = \cos(F(\eta))u_0^{(1)} + \sin(F(\eta))u_0^{(2)}, \tag{39b}$$

$$u^{(2)}(\eta) = -\sin(F(\eta))u_0^{(1)} + \cos(F(\eta))u_0^{(2)}, \tag{39c}$$

$$u^{(3)}(\eta) = u_0^{(3)}, \tag{39d}$$

where

$$F(\eta) = \sigma(\arctan\left(l_+(\eta)\right) - \arctan\left(l_-(\eta)\right) + D_5) \tag{40a}$$

$$D_5 = \arctan\left(l_-(0)\right) - \arctan\left(l_+(0)\right), \tag{40b}$$

$$l_\pm(\eta) = \frac{D_2e^\eta \pm (r_G/2)^2}{\sqrt{D_1D_2 - (r_G/2)^4}}. \tag{40c}$$

Hence, an arbitrary vector is rotated around $\mathbf{e}_{(3)}$ by an angle of $F(\eta)$ with respect to the local rest frame at the destination point $x_1^\mu(\eta)$ if isometrically transformed along the Killing vector field ξ_1^μ. The solution for the vector field ξ_4^μ is now trivial. As this transformation only yields an angular offset of $\Delta\varphi = \pi/2$, eq. (31b), the solution to the equations of isometric transport of vectors (36) is identical to the solution for the vector field ξ_1^μ, eq. (39). With these results we are able to map the special solution of the geodesic equations, Sec. III A, onto the general solution as presented in Sec. III B by means of isometrically transforming initial conditions.

V. MAPPING OF ARBITRARY CURVES

In this section, we will use finite isometric transformations to map several classes of curves. In this way, the general solution to the geodesic equations will be reproduced, the Gödel horizon for different observers will be calculated, and a non-circular class of CTCs will be generated.

A. Mapping of geodesics

With the results of the previous section, we are able to generate the solution of the geodesic equations, eqns. (24d), using geodesics starting at the origin [36] and finite isometric transformations.

Consider an arbitrary initial position x_0^μ and any lightlike or timelike local initial direction $u_0^{(a)}$. First, we rotate these initial conditions around the z-axis using the Killing vector field ξ_2^μ until $\varphi = \pi/2$. This step is necessary because only then the initial position can be isometrically translated to the origin using ξ_1^μ (compare Fig. 8). After this rotation by $\Delta\varphi = \pi/2 - x_0^\varphi$, we use the solution to the equations of isometric transport for ξ_1^μ, eqns. (30), to reach $r = 0$. Solving eq. (30b) for η yields

$$\eta_1 = \ln\left(\frac{r_G^2/2}{r_0^2 + r_G^2/2 + r_0\sqrt{r_0^2 + r_G^2}}\right). \tag{41}$$

Finally, we translate the resulting point to $z = 0$ using the Killing vector ξ_3^μ. The isometrically transformed initial direction is then found by inserting η_1 into eqns. (39). In this way, the local initial direction is rotated by an angle $\alpha = F(\eta_1)$, eq. (40a).

These initial conditions, $\bar{x}_0^\mu = (x_0^t, 0, \pi/2, 0)$ and the rotated local direction $u^{(a)}(\eta_1) = \bar{u}_0^{(a)}$ are then inserted into the special solution of the geodesic equations, eqns. (19). The resulting geodesic is then isometrically transformed back using the above transformations inverted and in reverse order. Inserting these results in the appropriate equations, finite isometric transformations for points and vectors as well as the special solution to the geodesic equations reproduces the general solution of Sec. III B.

Obviously, general solutions of the geodesic equations can be mapped onto other general solutions as well. Therefore, we consider arbitrary initial conditions as above and a desired destination position x_1^μ. The component x_0^μ is rotated around the z-axis until $\varphi = \pi/2$ is reached, isometrically translated along ξ_1^μ to map onto the desired radial coordinate $r = x_1^r$, then rotated to the destination angular coordinate $\varphi = x_1^\varphi$, and finally isometrically translated in time and the z-coordinate to arrive at x_1^μ. Again, the initial direction is only rotated due to the Killing vector field ξ_1^μ by an angle $F(\tilde{\eta}_1)$, where

$$\tilde{\eta}_1 = \ln\left(\frac{r_1^2 + r_G^2/2 + r_1\sqrt{r_1^2 + r_G^2}}{r_0^2 + r_G^2/2 + r_0\sqrt{r_0^2 + r_G^2}}\right). \tag{42}$$

Numerical implementations of this procedure and the general solution to the geodesic equations yield identical results.

B. Mapping of the Gödel horizon

Because Gödel's universe is homogeneous, every observer $\mathbf{O}, \mathbf{A}$ or $\mathbf{B}$ can legitimately declare his position as the origin of a coordinate system, where the line element takes the form of eq. (1). This definition yields an equivalent formulation of the Gödel horizon. Fig. 4 indicates how these horizons are shaped. The Gödel horizon around any point is the convex hull of all lightlike geodesics starting there. Furthermore, the horizon itself is a closed null curve (CNC), because $ds^2 = 0$ along the Gödel radius. We could use the general solution to the geodesic equations to calculate the exact shape. However, the usage of finite isometric transformations is by far more elegant.

Due to the homogeneity of the spacetime, each observer states that 'his' horizon is circular within the (xy)-plane. Fig. 10 shows three different horizons. Each horizon is depicted with respect to the coordinate system of the observer $\mathbf{O}$. The observer $\mathbf{A}$ results from an isometric transport of $\mathbf{O}$ along ξ_4^μ with $\eta = \eta_1$, eq. (41), and using $r_0 = r_G$. Observer $\mathbf{B}$ is subject to a similar transformation, where $\eta = 2\eta_1$.

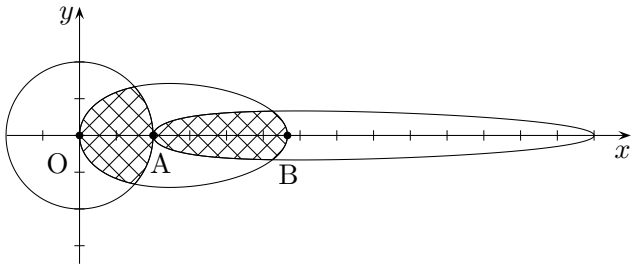

FIG. 10: Three horizons of three different observers $\mathbf{O}, \mathbf{A}$ and $\mathbf{B}$. Crosshatched regions mark common causality regions. Note that $\mathbf{O}$ and $\mathbf{B}$ do not share a common region.

We find that observer $\mathbf{O}$ and $\mathbf{A}$ share a common causality region marked by the left crosshatched area. A traveler $\mathbf{T}$ moving arbitrarily in this region will not travel through time from both observers' perspectives. Observers $\mathbf{A}$ and $\mathbf{B}$ share a similar region, but the horizons $\mathbf{O}$ and $\mathbf{B}$ are merely tangential to each other. Hence, motion restricted to the horizon around $\mathbf{O}$ can be causality violating but not visible for the observer $\mathbf{B}$. Furthermore, only the observer $\mathbf{A}$ is jointly visible to the observer $\mathbf{O}$ as well as $\mathbf{B}$. Note that each horizon is circular for the corresponding observer and only appears deformed due to the distortion caused by the chosen set of coordinates.

C. Mapping of worldlines and generation of CTCs

In this section we will discuss how worldlines are isometrically transformed. This will be used to generate interesting closed timelike curves (CTCs) from a circular set of worldlines, where $t(\lambda)$ is constant.

1. *Circular CTCs*

In Sec. II A, we reviewed that the light cones beyond the Gödel horizon intersect the $t = \text{const.}$ plane. A traveler can propagate into his own local future but into the past of an observer located at the origin of the coordinate system (compare Fig. 2). These CTCs are circles with constant coordinate time

$$x^t = \text{const},\ x^r = R = \text{const},\ x^\varphi = \omega\tau,\ x^z = 0, \tag{43}$$

where $R \geq r_G$. We generate CTCs when we require that u^t is zero. To find the corresponding direction in the local frame of reference, eqns. (12), we transform a local vector to the coordinate representation:

$$u^t = \frac{1}{c}u^{(0)} - \frac{\sqrt{2}r}{r_G c}\frac{1}{\sqrt{1 + (r/r_G)^2}}u^{(2)}, \tag{44a}$$

$$u^r = \sqrt{1 + (r/r_G)^2}\,u^{(1)}, \tag{44b}$$

$$u^\varphi = \frac{1}{r\sqrt{1 + (r/r_G)^2}}u^{(2)}, \tag{44c}$$

$$u^z = u^{(3)}. \tag{44d}$$

The circular CTCs are then constructed when setting $u^t = u^r = u^z = 0$ in the equations above. This results in a local timelike four-velocity $u^{(a)} = (\gamma c, 0, \gamma v_\varphi, 0)$, where the spatial velocity is given by

$$v_\varphi = c\sqrt{\frac{1}{2}[(r_G/R)^2 + 1]} \leq c, \tag{45}$$

and the non-zero component of the four-velocity u^μ is

$$u^\varphi = \omega = \frac{c}{R}\frac{1}{\sqrt{(R/r_G)^2 - 1}}. \tag{46}$$

Inserting the four-velocity into the Lagrangian, eq. (6), proves that this four-velocity is indeed a timelike vector. The four-acceleration is obtained using eq. (4), and the only non-zero component turns out to be

$$a^r = \omega^2 R\left\{[(R/r_G)^2+1][2(R/r_G)^2-1]\right\}, \tag{47}$$

which is positive $\forall\, R > r_G$. Hence, the traveler has to accelerate radially outwards to sustain the circular motion on the CTC. Note that there exists only one angular velocity ω for each radius $R > r_G$ to form a CTC. Other values of ω generate possible but non-closed worldlines. These worldlines are not causality violating and are comparable to the helix segment of the CTC in Fig. 2. From these results we calculate the Fermi-Walker transport of an arbitrary vector X^μ, eq. (5), and obtain the coupled system of linear differential equations

$$\dot{X}^t(\tau) = -X^r(\lambda)\frac{\sqrt{2}R^2}{\sqrt{R^2-r_G^2}(R^2+r_G^2)}, \tag{48a}$$

$$\dot{X}^r(\tau) = \quad X^t(\lambda)\frac{\sqrt{2}c^2R^2(R^2+r_G^2)}{r_G^2(R^2-r_G^2)^{3/2}}, \tag{48b}$$

$$\dot{X}^\varphi(\tau) = \quad X^r(\lambda)\frac{2cR^2r_G}{(R^2-r_G^2)^{3/2}(R^2+r_G^2)}, \tag{48c}$$

$$\dot{X}^z(\tau) = 0. \tag{48d}$$

With the abbreviations

$$B_{12} = -\frac{\sqrt{R^2-r_G^2}r_G}{c(R^2+r_G^2)}, \tag{49a}$$

$$B_{13} = \frac{\sqrt{2}r_G^2}{(R^2+r_G^2)\sqrt{R^2-r_G^2}}, \tag{49b}$$

$$\tag{49c}$$

the integration yields

$$X^t(\tau) = B_{12}\left[E_2\cos(\nu\tau) - E_1\sin(\nu\tau)\right], \tag{50a}$$

$$X^r(\tau) = E_2\sin(\nu\tau) + E_1\cos(\nu\tau), \tag{50b}$$

$$X^\varphi(\tau) = B_{13}\left[E_2\cos(\nu\tau) - E_1\sin(\nu\tau)\right] + E_3, \tag{50c}$$

$$X^z(\tau) = E_3\lambda, \tag{50d}$$

where

$$\nu = \frac{\sqrt{2}cR^2}{r_G(r_G^2-R^2)}. \tag{51}$$

Before determining the integration constants E_i, we formulate this solution with respect to a local comoving frame. First, eqns. (50) are expressed using the local rest frame, eqns. (12), denoted as $X^{(a)}$. To transform this intermediate result into a local comoving frame, we only have to apply a Lorentz boost. Obviously, the traveler $\mathbf{T}$ is moving in the $e_{(2)}$-direction of the rest frame. Hence, to transform the Fermi-Walker transported vector into the comoving frame of the moving observer $\mathbf{T}$, we apply a Lorentz boost to $X^{(a)}(\tau)$ in the same direction with $\beta = v_\varphi/c$ (compare eq. (45)). To express the fact that the comoving frame results from a Lorentz transformation $\Lambda_{(a)(b)}$ of the local rest frame, we designate the resulting vector as $X^{(a_\Lambda)}$. Then, the local initial conditions $X^{(a_\Lambda)}(0) = X_0^{(a_\Lambda)}$ fix the integration constants. The result of this calculation is

$$X^{(0_\Lambda)}(\tau) = \quad X_0^{(0_\Lambda)}, \tag{52a}$$

$$X^{(1_\Lambda)}(\tau) = \quad X_0^{(1_\Lambda)}\cos(\nu\tau) + X_0^{(2_\Lambda)}\sin(\nu\tau), \tag{52b}$$

$$X^{(2_\Lambda)}(\tau) = -X_0^{(1_\Lambda)}\sin(\nu\tau) + X_0^{(2_\Lambda)}\cos(\nu\tau), \tag{52c}$$

$$X^{(3_\Lambda)}(\tau) = \quad X_0^{(3_\Lambda)}. \tag{52d}$$

With these results at hand we consider the special case $X_0^{(a_\Lambda)} = (0,1,0,0)$ and calculate the rotation angle α after one orbit. After one period we have $\omega\tau_\circ = 2\pi$ and obtain

$$\tau_\circ = \frac{2\pi R}{c}\sqrt{(R/r_G)^2-1}, \tag{53a}$$

$$\alpha = \nu\tau_\circ = -\frac{2\sqrt{2}\pi(R/r_G)^3}{\sqrt{(R/r_G)^2-1}}, \tag{53b}$$

where we have used ω from eq. (46) In the limit $R \to r_G$ we obtain a closed null curve (CNC), where the spatial components describe the Gödel horizon. The local velocity of the corresponding photon, eq. (45), is c (as expected) and the proper time $\tau_\circ$, eq. (53a), converges to zero. However, a photon has to be forced on a circular orbit, because this curve does not represent a geodesic. This could be achieved, e. g., using an appropriate arrangement of mirrors.

2. Mapping of CTCs

This set of CTCs can now be mapped onto CTCs which pass through the origin. We transport a circular CTC along the Killing vector field ξ_4^μ, eq. (14c). Using an approach similar to the mapping of geodesics, Sec. V A, we calculate the isometric transformation of the point $x^\mu = (t_0, R, \pi, 0)$ to the origin, arriving at the same curve parameter η_1, eq. (41), which is now used in the solution to the equations of transport for ξ_4^μ, eqns. (31). The same transformation is applied to each point of the worldline. The resulting behavior can be anticipated when analyzing Fig. 8 and Fig. 9. The distance of lines of finite isometric transport, Fig. 8, decreases for larger distances to the origin. Hence, we expect that the transformed circle must appear deformed; resulting in a smaller radius of curvature for those parts of the worldline now distant from the origin. Fig. 9 reveals that the coordinate time values of one semi-cycle will be pushed to negative values while the other semi-cycle will experience a shift to positive values. This expected qualitative behavior is verified by the results shown in Fig. 11 and 12.

Apparently, the results of the previous section, which have been formulated with respect to a local frame, are still valid.

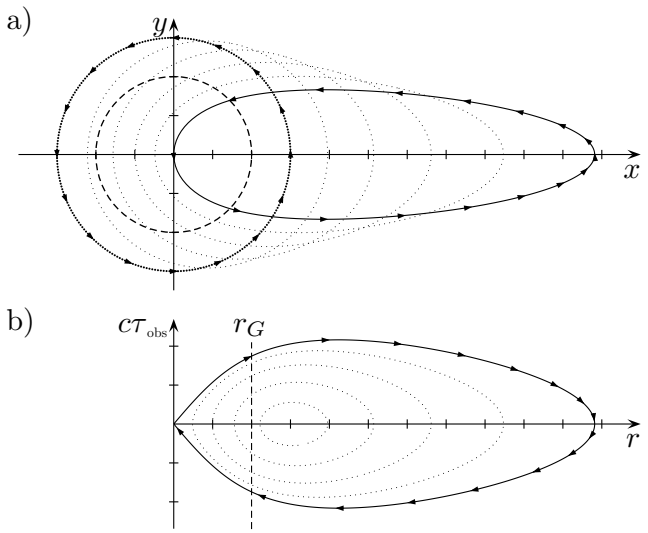

FIG. 11: Isometrically transporting a circular CTC of radius $R = 3r_G/2$ (densely dotted circle) along the Killing vector field ξ_4^μ in positive x-direction. In Fig. 11a sparsely dotted curves represent the isometric transport and each of these dotted curves is a CTC itself. Arrowheads indicate the traveler's flight direction. The resulting CTC (solid curve) represents a traveler starting at the origin, moving beyond the Gödel horizon – indicated as dashed circle in Fig. 11a or dashed line in Fig. 11b – and returning to the origin at the coordinate time of departure. Fig. 11b: Observer time as a function of the radial coordinate of the CTC. Note that coordinate time coincides with the proper time of a resting observer **O**. Therefore, the traveler **T** is moving back in time from the resting observer's perspective. Also note that $dt/d\lambda > 0$ as long as $r < r_G$.

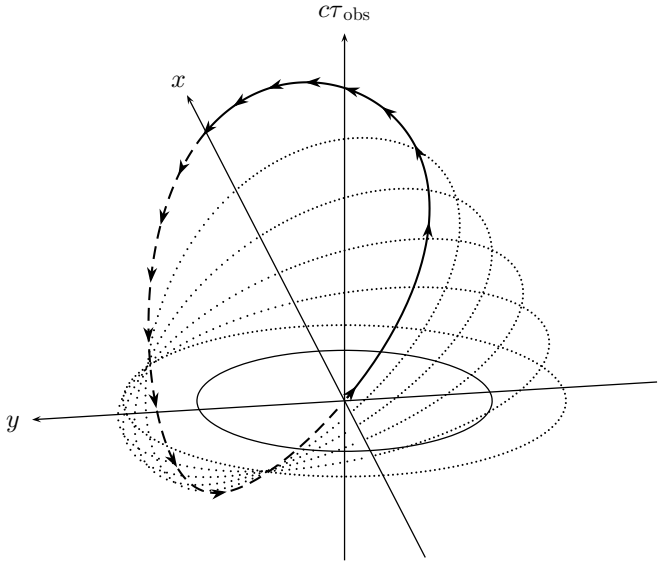

FIG. 12: Three-dimensional presentation of Fig. 11(a). Isometrically transporting a circular CTC does not only result in a different spatial appearance but affects the time coordinate as well. Dashed or sparsely dotted curve segments are below the xy-plane, solid or densely dotted curve parts have $t = \tau_{\rm obs} \geq 0$. The Gödel horizon is shown as solid circle.

VI. CONCLUSION

We have derived analytical solutions to the geodesic equations of Gödel's metric for special and general initial conditions. The general solution was used to determine whether or not causality violations exist when traveling on geodesics. A lightlike or massive paricle travels back in time if the initial velocity is $v \gtrsim 0.980172c$ and the initial radial coordinate is $r_0 \lesssim 1.7r_G$. For a maximum time interval $\Delta T^v_{\rm min}$, a single particle would exist twice within the Gödel horizon. In all cases, causality is not violated. The equations of isometric transport for both points and directions were solved for all five Killing vector fields. Special solutions to the geodesic equations and finite isometric transformations could be combined to generate the general solution of the geodesic equations. After mapping the Gödel horizon we depicted regions of common causality for different observers. Then, we described circular CTCs and calculated the Fermi-Walker transport along these circular lines with $R > r_G$. An observer traveling on these curves has to accelerate radially outwards and, after a proper time $\tau_\circ$ of one period, will be rotated by an angle α (see eqns. (53)). We then isometrically transformed these circles to create CTCs starting at the origin. This resulted in a time travel starting at the origin. Observer **O** can therefore see the time traveler **T**, who would otherwise be hidden beyond the optical horizon r_G. Because these CTCs are created using isometric transformations, eqns. (53) remain valid.

The correctness of the solution of the geodesic equations, both special and general, has been verified by comparisons with numerical calculations using, e. g., a fourth-order Runge-Kutta integrator or the integrators provided by the Gnu Scientific Library (*GSL*). A verification of the analytical solutions to the equations of isometric transport for points as well as vectors has been achieved through comparisons of mapped special solutions and the general solution of the geodesic equations.

As an outlook, one could think of calculating the parallel transport for an arbitrary vector, which is transported along a geodesic starting at the origin. Then, one could directly specify the general solution to this problem using finite isometric transformations. To which extent the results presented carry over to the case where pertubations are introduced in Gödel's metric, such as those considered by Barrow and Tsagas [12], remains an open question, which should be clarified by future work.

In this paper, we have discussed CTCs. These investigations can be generalized to PTCs and to curves closed in time but not necessarily in space. These can be used, together with the analytical solution to the equations of isometric transport, for an egocentric visualization as has been done by us in [22].

Acknowledgments

We thank the DFG (German Research Foundation) for the financial support of the project "Visualisierung geschlossener zeitartiger Kurven in der Allgemeinen Relativitätstheorie" (project number: 99015432).

Appendix A: Appendixes

1. Solution of the geodesic equations

Considering the equations of motion (8), we realize that the radial equation (8b) is solely dependent on the radial coordinate and its derivative. The other three equations (8a), (8c) and (8d) require the solution of the radial equation. Hence, we solve the radial equation and use the result to solve the remaining equations. Obviously, these steps can also be used for the geodesic equations for special initial conditions, eq. (17).

a. Special initial conditions

After separation of variables in the radial equation, eq. (17b), we obtain

$$\frac{\pm dr}{\sqrt{r_G^2 K_+/K_- - r^2}} = \frac{\sqrt{K_-}}{r_G}\, d\lambda, \tag{A1}$$

where the two signs on the left-hand side result from extracting the root of eq. (17b) and describe a photon leaving from or arriving at the origin, respectively. This equation is integrated, which yields

$$\pm \arcsin\left(\frac{r}{r_G}\sqrt{\frac{K_-}{K_+}}\right) - r_0 = \frac{\sqrt{K_-}}{r_G}(\lambda - \lambda_{0\pm}) \tag{A2}$$

with two different integration constants $\lambda_{0\pm}$, which depend on the branch of the solution. Furthermore we set $r_0 = 0$ due to our initial conditions. This can be written as

$$r(\lambda) = \pm r_G \sqrt{\frac{K_+}{K_-}} \sin\left(\frac{\sqrt{K_-}}{r_G}(\lambda - \lambda_{0\pm})\right). \tag{A3}$$

The different branches of the solution are merged to a continuous function for both incoming and outgoing photons and the initial condition r_0 which directly results in eq. (19b).

After inserting eq. (19b) into (17a) we find

$$c\dot{t} = -k_0 \frac{K_-/K_+ - \sin^2\left(\sqrt{K_-}/r_G\,\lambda\right)}{K_-/K_+ + \sin^2\left(\sqrt{K_-}/r_G\,\lambda\right)}. \tag{A4}$$

An integral for this equation is given by

$$ct(\lambda) = k_0\lambda + \sqrt{2} r_G \arctan\left(\frac{k_0\sqrt{2}}{\sqrt{K_-}} \tan\left(-\frac{\sqrt{K_-}}{r_G}\lambda\right)\right). \tag{A5}$$

Because $\arctan(\tan(y))$ is a sawtooth function, the floor function $p_q(\lambda)$ as in eq. (20a) is introduced. Including the integration constant t_0, we obtain a continuously differentiable function $t(\lambda)$ as in eq. (19a).

The angular equation (17c) is also solvable after inserting the radial solution (19b). The result is

$$\dot{\varphi} = \frac{-\sqrt{2}k_0 K_-/K_+}{r_G\left[K_-/K_+ + \sin^2\left(\sqrt{K_-}/r_G\lambda\right)\right]}. \tag{A6}$$

The integral reads

$$\varphi(\lambda) = \arctan\left(\frac{k_0\sqrt{2}}{\sqrt{K_-}} \tan\left(-\frac{\sqrt{K_-}}{r_G}\lambda\right)\right), \tag{A7}$$

where we again need the floor function $p_q(\lambda)$ to generate a continuously differentiable function. Including the integration constant φ_0 we obtain the solution, eq. (19c).

Eq. (17d) is trivial. For investigating geodesics starting at the origin, we set the integration constant $z_0 = 0$.

b. General initial conditions

We substitute $R = r/r_G$ in the general radial geodesic equation (8b). After separation of variables, we see that

$$\int_{R(0)}^{R(\lambda)} \frac{u\,du}{\sqrt{-B_1 u^4 + B_3 u^2 + B_2}} = (\pm\lambda - \lambda_0). \tag{A8}$$

After substituting $u^2 = v$, we can solve this equation using standard integration tables [37], viz.

$$\int \frac{dx}{\sqrt{X}} = \frac{-1}{\sqrt{-a}} \arcsin\left(\frac{2ax+b}{\sqrt{b^2-4ac}}\right), \tag{A9}$$

where $X = ax^2 + bx + c$. It is necessary, however, that $B_1 > 0$ and $B_3^2 + 4B_1B_2 > 0$. This is achieved through using the initial conditions, eq. (13) combined with all possible choices of local initial directions. The estimate necessary is omitted here because the calculation does not yield any physical insight.

We calculate the above integral, solve for $R(\lambda)$, and neglect the negative branch resulting form extracting the root. To decide the algebraic sign in $\pm\lambda$, we discuss the monotonic behavior of the solution. For instance, a geodesic starting radially outwards must be monotonically increasing in r for small λ. We find that radially outgoing geodesics require the negative sign and vice versa. Hence, we substitute $\pm\lambda \to -\sigma_1\lambda$. We arrive at the radial solution, eq. (24b), after determining the integration constant C_1 using $r(0) = r_0$.

To solve the angular equation (8c), we insert the radial solution (eq. (24b)). After several steps of simplification we find, using $\bar{B} = \sqrt{B_3^2 + 4B_1B_2}$,

$$\begin{aligned}\dot{\varphi}(\lambda) &= \frac{2B_1k_2/r_G^2}{B_3 - \bar{B}\sin(v(\lambda)/2)} \\ &\quad - \frac{2B_1k_2/r_G^2 + 2\sqrt{2}k_0B_1/r_G}{2B_1 + B_3 - \bar{B}\sin(v(\lambda)/2)},\end{aligned} \tag{A10}$$

where we used the abbreviations (eq. (21)) and the auxiliary function $v(\lambda)$ (eq. (23a)). Both terms can be integrated using [38]

$$\int \frac{dx}{b+d\sin(ax)} = \frac{2}{a^2\sqrt{b^2-d^2}} \times \arctan\left(\frac{b\tan(ax/2)+d}{\sqrt{b^2-d^2}}\right), \quad \text{(A11)}$$

where $b^2 > d^2$ is required. Again, this can be shown using eqns. (13) and all possible choices of lightlike and timelike local vectors. Prefactors $2/(a^2\sqrt{b^2-d^2})$ are simplified considerably when using $y/\sqrt{y^2} = \mathrm{sgn}(y)$, the integration constant is found when setting $\varphi(0) = \varphi_0$, and after a lengthy calculation the solution, eq. (24c), is found.

The time equation (8a) is solved analogously. Again, we use the radial solution (eq. (24b)), the abbreviations B_i, the auxiliary function $v(\lambda)$, and obtain the following equation:

$$c\dot{t} = \frac{k_0(-2B_1+B_3)-2\sqrt{2}B_1k_2/r_G}{2B_1+B_3-\bar{B}\sin(v(\lambda)/2)} - \frac{k_0\bar{B}\sin(v(\lambda)/2)}{2B_1+B_3-\bar{B}\sin(v(\lambda)/2)}. \quad \text{(A12)}$$

The first term is integrated using eq. (A11), the second term requires the formula [39]

$$\int \frac{\sin(ax)dx}{b+d\sin(ax)} = \frac{x}{d} - \frac{b}{d}\int \frac{dx}{b+d\sin(ax)}. \quad \text{(A13)}$$

Again, $b^2 > d^2$ is necessary and fulfilled. After simplifications similar to those used in the angular solution, we have to introduce the periodicity function $\tilde{p}(\lambda)$, eq. (23d), for continuously differentiable temporal behavior. Requiring $t(0) = t_0$ determines the integration constant C_3 as in our solution, eq. (24a).

2. Isometric transformations along non-trivial Killing vector fields

a. *Transformation of points*

The equations of isometric transport (29) for the Killing vector field ξ_1^μ (eq. (14b)) read

$$\frac{dt}{d\eta} = \frac{r}{\sqrt{2}c\sqrt{1+(r/r_G)^2}}\cos\varphi, \quad \text{(A14a)}$$

$$\frac{dr}{d\eta} = \frac{r_G}{2}\sqrt{1+(r/r_G)^2}\sin\varphi, \quad \text{(A14b)}$$

$$\frac{d\varphi}{d\eta} = \frac{r_G[1+2(r/r_G)^2]}{2r\sqrt{1+(r/r_G)^2}}\cos\varphi, \quad \text{(A14c)}$$

$$\frac{dz}{d\eta} = 0, \quad \text{(A14d)}$$

where both r and φ are dependent of η. We solve eq. (A14b) for φ, i. e.

$$\varphi = \arcsin\left(\frac{2\dot{r}}{r_G\sqrt{1+(r/r_G)^2}}\right). \quad \text{(A15)}$$

All differentiations in this section are with respect to the isometric parameter η. By inserting this equation into eq. (A14c) we obtain an uncoupled differential equation. Using $(d\arcsin(x))/(dx) = 1/\sqrt{1-x^2}$ and $\cos(\arcsin(x)) = \sqrt{1-x^2}$ we finally arrive at

$$4r_G r\ddot{r} + 4r^3\ddot{r} + 4r^2\dot{r}^2 - 3r_G^2r^2 + 4r_G^2\dot{r}^2 - 2r^4 - 2r_G^4 = 0. \quad \text{(A16)}$$

After substituting $y = r^2$ we find that

$$(r_G^2 + y^2)(\ddot{y} - y - r_G^2/2) = 0. \quad \text{(A17)}$$

Because y is real, we neglect the first factor and obtain

$$\ddot{y} - y = r_G^2/2, \quad \text{(A18)}$$

which is solved by

$$y(\eta) = D_1e^{-\eta} + D_2e^{\eta} - r_G^2/2. \quad \text{(A19)}$$

Eq. (30b) is reproduced after the back substitution $r = \sqrt{y}$.

The solution $\varphi(\eta)$, eq. (30c), results from inserting $r(\eta)$ and its derivative $\dot{r}(\lambda)$ into eq. (A15).

Both $r(\eta)$ and $\varphi(\eta)$ are inserted into eq. (A14a), which can then be written as

$$\dot{t} = \frac{\sqrt{2}r_G\sqrt{D_1D_2-(r_G/2)^2}}{c(D_1e^{-\eta}+D_2e^{\eta}+r_G^2/2)}. \quad \text{(A20)}$$

After the substitution $e^\eta = h$, $dh/d\eta = e^\eta$ we arrive at

$$\frac{dt}{dh} = \frac{\sqrt{2}r_G\sqrt{D_1D_2-(r_G/2)^4}}{c(h^2D_2+hr_G^2/2+D_1)}, \quad \text{(A21)}$$

which is solved with the appropriate arctan function. After the back substitution, the solution eq. (30a) is found. The integration constants D_1, D_2, D_3 and D_4, eqns. (33), are determined using the initial conditions $x^\mu(0) = x_0^\mu$. This choice also ensures that the solution is well-behaved, i. e. $D_1D_2-(r_G/2)^4 > 0\,\forall x_0^\mu$. Note that eq. (A15) is only valid if φ is in the right half plane. For $\varphi \in]\frac{\pi}{2}, \frac{3\pi}{2}[$, we need a different branch of the arcsin-function which results in the parameter σ to distinguish both half planes, see eq. (32).

The solution of eq. (14c) can be derived from the solution of eq. (14b). Considering eq. (14) it is obvious [2] that $\xi_4(\varphi) = \xi_1(\varphi-\pi/2)$. Hence, the solution of eq. (14c) is obtained via shifting the angular coordinate in eq. (30) by $+\pi/2$ as stated in eq. (31).

b. Transformation of vectors

The equations of isometric transport for vectors (36) for the Killing vector field ξ_1^μ (eq. (14b)) are given by eqns. (38). To formulate these equations with respect to the local frame of reference (eq. (12)), we consider an arbitrary vector $\mathbf{u} = u^\mu \partial_\mu = u^{(a)} \mathbf{e}_{(a)}$. As both u^μ and $u^{(a)}$ depend on the curve parameter η we find that (using eq. (37))

$$u^t = -\frac{r\sqrt{2}}{c\tilde{q}(r)}\, u^{(2)} + \frac{1}{c} u^{(0)}, \tag{A22a}$$

$$u^r = \frac{\tilde{q}(r)}{r_G} \quad u^{(1)}, \tag{A22b}$$

$$u^\varphi = \frac{r_G}{r\tilde{q}(r)} \quad u^{(2)}, \tag{A22c}$$

$$u^z = \quad u^{(3)}, \tag{A22d}$$

and

$$\dot{u}^t = \frac{\sqrt{2}}{c\tilde{q}(r)} \left(\frac{r^2 \dot{r}}{q^2(r)} u^{(2)} - \dot{r} u^{(2)} - r \dot{u}^{(2)} \right) + \frac{1}{c} \dot{u}^{(0)}, \tag{A23a}$$

$$\dot{u}^r = \frac{r\dot{r}}{r_G \tilde{q}(r)} u^{(1)} + \frac{\tilde{q}(r)}{r_G} \dot{u}^{(1)}, \tag{A23b}$$

$$\dot{u}^\varphi = \frac{r_G}{\tilde{q}(r)} \left(\frac{\dot{u}^{(2)}}{r} - \frac{\dot{r}}{r^2} u^{(2)} - \frac{\dot{r}}{q^2(r)} u^{(2)} \right), \tag{A23c}$$

$$\dot{u}^z = \dot{u}^{(3)}, \tag{A23d}$$

where the derivative is with respect to η. We insert eqns. (A22) and (A23) in eqns. (38) and solve for the derivative of the local formulation $\dot{u}^{(a)}$. Note that r and φ are evaluated along the solution (30), i. e. $r = r_1(\eta)$ and $\varphi = \varphi_1(\eta)$. Then, the equations of transport (38) become

$$\dot{u}^{(0)} = \quad 0, \tag{A24a}$$

$$\dot{u}^{(1)} = \quad f(\eta) u^{(2)}, \tag{A24b}$$

$$\dot{u}^{(2)} = -f(\eta) u^{(1)}, \tag{A24c}$$

$$\dot{u}^{(3)} = \quad 0, \tag{A24d}$$

with

$$f(\eta) = \frac{r_G^2 \cos\varphi_1(\eta)}{2 r_1(\eta) \tilde{q}(r_1(\eta))} = \frac{r_G^2 \sqrt{D_1 D_2 - (r_G/2)^4}}{r_1^2(\eta)[r_G^2 + r_1^2(\eta)]}. \tag{A25}$$

Hence, both components $u^{(0)}$ and $u^{(3)}$ remain unchanged during transport, while $u^{(1)}$ and $u^{(2)}$ are rotated around the local $\mathbf{e}_{(3)}$ axis. Analytical solutions to these equations can be found when using an ansatz specific to the rotational symmetry and applying the variation of constants method. The extension reads

$$u^{(1)}(\eta) = \; D_6 \cos(F(\eta)) + D_7 \sin(F(\eta)), \tag{A26a}$$

$$u^{(2)}(\eta) = -D_6 \sin(F(\eta)) + D_7 \cos(F(\eta)), \tag{A26b}$$

where

$$F(\eta) \; = \; \int f(\eta') d\eta' + D_5. \tag{A27}$$

The integration of $f(\eta)$ and the determination of D_5 using $F(0) = 0$ reproduce the solution as shown in eq. (40). Note that the parameter σ, eq. (32), ensures the correct behavior for both half planes. The integration constants D_6 and D_7 correspond to the components $u_0^{(1)}$ and $u_0^{(2)}$ of the initial vector with respect to the local frame of reference, respectively.

Again, we can derive the solution for the Killing vector field ξ_4^μ (eq. (14c)) using this solution for the Killing vector field ξ_1^μ. Because the finite transport for points only yields a constant angular shift of $\Delta\varphi = +\pi/2$, which, in particular, is independent of the curve parameter η, the solution using ξ_4^μ is identical to this solution for ξ_1^μ.

3. Estimates

For curiosity, we provide estimates of characteristics of the Gödel universe taking into account a) estimates for the cosmological constant and b) best-fit approximations from the *WMAP* data.

a. Gödel's universe and the cosmological constant

The cosmological constant Λ is limited to

$$|\Lambda| < 10^{-51} \frac{1}{\mathrm{m}^2} \tag{A28}$$

due to cosmological observations [26]. In Gödel's universe, the cosmological constant is related to the Ricci scalar [1] and reads

$$\Lambda = \frac{R}{2} = -\frac{2}{r_G^2}. \tag{A29}$$

Note that Gödel [1] used the field equations in the form $G_{\mu\nu} = \sigma T_{\mu\nu} + \Lambda g_{\mu\nu}$ whereas we use $G_{\mu\nu} + \Lambda g_{\mu\nu} = \sigma T_{\mu\nu}$. This convention results in a different sign for the cosmological constant. Eq. (A29) determines the minimal Gödel radius, which is

$$r_G \approx 4.47 \times 10^{25} \mathrm{m} \approx 0.35\, r_{\mathrm{univ}}, \tag{A30}$$

where we set $r_{\mathrm{univ}} = 13.7 \times 10^9$ ly. The maximum time travel on lightlike geodesics, eq. (26), is

$$\Delta T^c_{\mathrm{min}} \approx -1.78 \times 10^8 \,\mathrm{a}. \tag{A31}$$

For circular CTCs with a radius $R = 2r_G$ and eq. (53a) we obtain a proper time

$$\tau_\circ \approx 1.02 \times 10^{11} \,\mathrm{a} \tag{A32}$$

for the round trip, where the local tetrad is rotated by an angle of

$$\alpha \approx -6.532 \times 360^\circ \tag{A33}$$

due to the Fermi-Walker transport, eq. (53b). The local velocity, eq. (45), is

$$v_\varphi \approx 0.79c. \tag{A34}$$

b. Gödel's universe and best-fit WMAP data

Barrow et. al. [28] derived upper limits for the rotation of the universe. Following the notation of that paper, Jaffe et. al. [29] and Bridges et. al. [30, 31] investigated, how Bianchi VII_h models can be fitted to the first-year and three-year WMAP data. They found that the best-fit approximation is achieved when using a very small rotation rate ω of the universe of roughly

$$\omega \approx 5 \times 10^{-10}\, H_0, \tag{A35}$$

where H_0 is the Hubble constant. We take $H_0 \approx 75\,(\mathrm{km/s})/(\mathrm{Mpc})$ and identify ω with the rotation scalar Ω_G (compare eq. (2)). Solving for the Gödel radius results in

$$r_G \approx 2.69 \times 10^9\, r_{\mathrm{univ}}. \tag{A36}$$

The values corresponding to the results of the last section read

$$\Delta T^c_{\mathrm{min}} \approx 1.3877 \times 10^{18}\,\mathrm{a}, \tag{A37a}$$

$$\tau_\circ \approx 8.03 \times 10^{20}\,\mathrm{a}, \tag{A37b}$$

while v_φ and α remain unchanged.

[1] K. Gödel, Reviews of Modern Physics **21**, 447 (1949).

[2] E. Kajari, R. Walser, W. P. Schleich, and A. Delgado, Gen. Rel. Grav. **36**, 2289 (2004).

[3] W. J. Stockum, Proc. Roy. Soc. Edinburgh **57**, 135 (1937).

[4] M. Visser, *Lorentzian Wormholes - From Einstein to Hawking* (Springer-Verlag New York, Inc., 1996).

[5] D. Birmingham and S. Sen, Phys. Rev. Lett. **84**, 1074 (2000).

[6] V. P. Frolov and I. D. Novikov, Phys. Rev. D **42**, 1057 (1990).

[7] S. DeDeo and J. R. Gott, Phys. Rev. D **66**, 084020 (2002).

[8] S. W. Hawking, Phys. Rev. D **46**, 603 (1992).

[9] J. Navez, Bulletin de la Société Royale des Sciences de Liège **39**, 470 (1970).

[10] A. K. Raychaudhuri and S. N. G. Thakurta, Phys. Rev. D **22**, 802 (1980).

[11] M. J. Rebouças and J. Tiomno, Phys. Rev. D. **28**, 1251 (1983).

[12] J. D. Barrow and C. G. Tsagas, Class. Quant. Grav. **21**, 1773 (2004).

[13] J. Pfarr, Gen. Rel. Grav **13**, 1073 (1981).

[14] V. M. Rosa and P. S. Letelier, Gen. Rel. Grav. **39**, 1419 (2007).

[15] D. Sahdev, R. Sundararaman, and M. S. Modgil, *The Gödel Universe: A Practical Travel Guide* (2006), URL `http://www.citebase.org/abstract?id=oai:arXiv.org:gr-qc/0611093`.

[16] W. Kundt, Z. Phys. **145**, 611 (1956).

[17] S. Chandrasekhar and J. P. Wright, Proc. Natl. Acad. Sci. U.S.A pp. 341–347 (1961).

[18] H. Stein, Philos. Sci. **37**, 589 (1970).

[19] I. Ozsváth and E. Schücking, Am. J. Phys. **71**, 801 (2003).

[20] M. Novello, I. D. Soares, and J. Tiomno, Phys. Rev. D **27**, 779 (1983).

[21] F. Grave and M. Buser, IEEE Transactions on Visualization and Computer Graphics **14**, 1563 (2008), ISSN 1077-2626.

[22] F. Grave, T. Müller, C. Dachsbacher, and G. Wunner, in *Computer Graphics Forum (Proc. Eurovis 09)*, edited by H.-C. Hege, I. Hotz, and T. Munzner (Blackwell Publishing, 2009), vol. 28 of *The International Journal of the Eurographics Association*, pp. 807–814.

[23] S. Feferman, ed., *Kurt Gödel: Collected Works, Vol. II* (Oxford University Press, 1995), ISBN 0-19-507255-3.

[24] B. D. B. Figueiredo, I. D. Soares, and T. J., Class. Quantum Grav. **9**, 1593 (1992).

[25] P. Marecki, in *Gödel type spacetimes: history and new developments*, edited by M.Scherfner and M.Plaue (in print, 2009).

[26] W. Rindler, *Relativity: Special, General, and Cosmological, 2nd edition* (Oxford University Press, 2006), ISBN 978-0-19-856732-8.

[27] H. Stephani, Allgemeine Relativitätstheorie. Eine Einführung in die Theorie des Gravitationsfeldes. H. Stephani. 3., neubearbeitete Auflage. Hochschulbücher für Physik **43** (1988).

[28] J. D. Barrow, Juszkiewicz, and D. H. Sonoda, Mon. Not. R. Astron. Soc. **213**, 917 (1985).

[29] T. R. Jaffe, A. J. Banday, H. K. Eriksen, K. M. Górski, and F. K. Hansen, ApJ **629**, L1 (2005).

[30] M. Bridges, J. D. McEwen, A. N. Lasenby, and M. P. Hobson, Mon. Not. R. Astron. Soc. **377**, 1473 (2007).

[31] M. Bridges, J. D. McEwen, M. Cruz, M. P. Hobson, A. N. Lasenby, P. Vielva, and E. Martínez-González, Mon. Not. R. Astron. Soc. **390**, 1372 (2008).

[32] I. Bronstein, K. Semendjajew, G. Musiol, and H. Mühlig, *Handbook of Mathematics* (Springer, 2007).

[33] In this work, we denote the projection onto a plane as a subspace.

[34] This is comparable to the Schwarzschild metric. Schwarzschild coordinates are interpreted as the coordinates for an observer resting with respect to spatial infinity.

[35] Time travel can only be realized if the geodesic is partially propagating beyond the horizon. To maximize the

part of the geodesic lying beyond the horizon, we must set $u_0^{(3)}$ to zero. Otherwise, the effective velocity in the (xy)-subspace is reduced and the geodesic becomes smaller in radial extend.

[36] More precisely, we only need geodesics with $\varphi_0 = z_0 = t_0 = 0$ and arbitrary k_3 in eqns. (19) to generate any geodesic. Due to the obvious symmetries of Gödel's universe, manifested in the trivial Killing vectors ξ_0, ξ_2 and ξ_3 (eqns. (14a)), all geodesics starting at the origin can be created using this subset.

[37] see [32], integral. (241).

[38] see [32], integral (306a).

[39] see [32], integral (307).